2016-01-01

Development Of The Thermal Wire Embedding Technology For Electronic And Mechanical Applications On Fdm-Printed Parts

Daniel Abraham Marquez
University of Texas at El Paso, dmarquez24@hotmail.com

DEVELOPMENT OF THE THERMAL WIRE EMBEDDING TECHNOLOGY FOR ELECTRONIC AND MECHANICAL APPLICATIONS ON FDM-PRINTED PARTS

DANIEL ABRAHAM MARQUEZ

Master's Program in Mechanical Engineering

APPROVED:

Ryan Wicker, Ph.D., Chair

Yirong Lin, Ph.D.

Eric MacDonald, Ph.D.

Charles Ambler, Ph.D.
Dean of the Graduate School

Dedication

This thesis is dedicated to my wife, daughters, and mother who have been my motivation to my continued education and have supported and encouraged me throughout the journey.

DEVELOPMENT OF THE THERMAL WIRE EMBEDDING TECHNOLOGY FOR ELECTRONIC AND MECHANICAL APPLICATIONS ON FDM-PRINTED PARTS

by

DANIEL ABRAHAM MARQUEZ, B.S.M.E.

THESIS

Presented to the Faculty of the Graduate School of

The University of Texas at El Paso

in Partial Fulfillment

of the Requirements

for the Degree of

MASTER OF SCIENCE

Department of Mechanical Engineering

THE UNIVERSITY OF TEXAS AT EL PASO

May 2016

Acknowledgements

I would like to express my gratitude to Dr. Ryan Wicker, the director of the W. M. Keck Center for 3D innovation at the University of Texas at El Paso (UTEP), my advisor, and committee chair in this work, for giving me the opportunity to allow me to be part of this type of work. Mr. David Espalin, the associate director and center manager of the W.M. Keck Center, for his continuous support, mentorship, and constructive criticism throughout my research as a graduate student. With David's guidance the development of my work was greatly impacted by his contribution. I would also like to extend my appreciation to my committee members, Dr. Eric MacDonald and Dr. Yirong Lin for taking their valuable time to be a part of my committee.

Several other people within the Keck Center deserve recognition. I would like to thank Mr. Alfonso Fernandez for his help in machining components, Mr. Jose Motta for his contribution in the programming and wiring of the electrical components onto a control box, Ms. Lluvia Herrera for her help with fabricating and testing the tensile test specimens, Mr. Chris Minjares for assisting in taking measurements and for designing and building the support structure needed in order to take measurements of embedded wires. Mr. Jose Gonzalez and Mr. Mohammad Hossain for their technical writing inputs. Also, I would like to thank the other faculty, staff, and students of the Keck Center for their support in this project.

Finally, I would like to thank my family for being the motivation for pursuing my graduate degree. In particular my amazing wife, April, my beautiful daughters, Averie, Amri, and Leslie, as well as my selfless mother, Irma, for their continuous support, encouragement, and sacrifice throughout my continued education.

Abstract

Additive Manufacturing (AM) has increased in popularity and attracted much attention from many fields such as automotive, aviation, aerospace, and even the fashion industry. Since the early 2000s, Fused Deposition Modeling (FDM) technologies have been the most popular in the AM world ("Wohlers Talk" Popularity of FDM). These technologies have been mainly used for building parts for prototype and structural type of applications such as a fixture for components or a housing for mechanisms.

With the current state of the FDM technologies, the functionality of the parts that are printed are limited to the applications listed before or simply just as visual aids. Adding more functionality to these structural parts allows the creation of end user parts which cannot be manufactured with traditional means of fabrication. Discussed in this work is the design and development of the thermal wire embedding (TWE) apparatus, describing three generations of the tool, each contains improvements to facilitate both wire embedding and maintenance. The TWE tool is designed to embed wires into the interlayers or surface of a FDM-built part. Adding conductive wires to an FDM-built part provides an electronic functionality to the design and due to the wires acting as a reinforcement, they inherently increase the mechanical properties of the part.

The TWE tool is fully automated to drive wire at various speeds with the use of a DC motor and cut wire with the aid of a cutting mechanism. The TWE tool is capable of embedding wire of different gauges as well as different materials. The TWE can place wires a close as 0.5 mm apart without seeing any shorting between the wires. With the ability to adapt to different motion control systems, the TWE tool can embed 28 AWG copper wires in different orientations with a measured accuracy as close as +/- 29 μm of its intended position. The ultimate goal of this line of research is to incorporate the TWE tool with multiple technologies to create a multi-functional AM printed part.

Table of Contents

List of Tables

List of Figures

Chapter 1: Introduction

1.1 BACKGROUND

Additive manufacturing (AM), or also more commonly known as 3D printing and rapid prototyping, is a relatively new automated fabrication process which has recently grown ever more popular than its earlier models developed in the 1980's. All technologies within 3D printing have the ability to manufacture parts directly from any computer-aided design (CAD) files. This process is accomplished by building the model in a layer by layer fashion. The result of these AM products have been found to be used as structural parts, tooling, niche products, prototypes, and even biomedical implants (Lansford, 2016.). The AM printed part's applications have been limited with the current state of the AM technologies. The limitations are within the parts functionality. The applications of the printed parts are generally used for prototyping, structural applications, or simply as visual aids.

The fabrication of objects through the deposition of a material, typically a polymer, using a print head nozzle technology is a commonly known form of 3D printing. Fused deposition modeling (FDM) is the most popular kind of AM technology, which uses a material extrusion process utilized to make thermoplastic parts through heated extrusion and deposition of materials layer by layer (ASTM F2792, 2015). These 3D printers can fabricate complex geometrical parts that may not be achieved with traditional means of fabrication such as subtractive manufacturing (i.e., milling, lathing) or casting. Although this is a great alternative for such complex geometrical parts, there are still several attributes required to be able to produce end-use products. Recently there have been many efforts focused into providing more functionality to FDM-printed models on top of them being used for structural applications. Some of the efforts to proving more functionality to FDM-printed parts will be discussed in the latter.

1.2 MOTIVATION

The FDM material extrusion process deposits material in a layer-by-layer fashion. Due to each layer being fabricated individually, the FDM building process can be interrupted in order to access these layers when necessary. These layers can be used to include additional features during intermediate steps. The research presented here takes advantage of these individual layers by developing a technology and method that will result with the embedding of wire patterns on the interlayers or exposed surfaces of an FDM-printed part. The development of this technology will ultimately be incorporated with the Multi^{3D} system. The Multi^{3D} system will evolve on the currently used FDM process as a whole by introducing fully automated technologies and enabling end use parts by adding multi functionality to the FDM-built part. Therefore, the main motivation of the present research is to develop an apparatus and method which will embed metal wires into these FDM-printed parts. These wires can be used for traces to connect electronic components, radiating elements for antennas, ground planes, wire bus, heat sinks, and as a mechanical reinforcement. In this work, three generations of the tool will be discussed, each containing improvements to facilitate both wire embedding and maintenance of the tool.

1.3 THESIS OBJECTIVES

There are 5 thesis objectives and are listed as follows:

1. Design and develop a technology that will result in wires to be encapsulated in the interlayers of 3D printed thermoplastic parts.

2. Incorporate a motion control system that consists of at least Cartesian XYZ linear motion travel.

3. Develop and evaluate a method that allows the wire embedding tool to embed wire in patterns seen in electronic applications.

4. Determine how the wire embedding apparatus modifies the mechanical properties of an FDM-printed part.

5. Determine the functionality of embedding wires in FDM-printed parts.

1.4 THESIS OUTLINE

The subsequent material was divided into 6 chapters. Chapter 2 is composed of a literature review of topics focusing on research conducted in order to develop multifunctional 3D printed parts, particularly by incorporating an electronic functionality. Chapter 2 will then go over an overview of the FDM technology and transition into research done in order to embed components into FDM-built parts. In Chapter 3, the design and methodology of the thermal wire embedding (TWE) prototype tool will be discussed. Chapter 4 consists of two design iterations of the TWE tool. Projects showcasing the TWE tool's applications will be discussed in Chapter 5, showing the versatility of the TWE tool's flexibility to different AWG wire sizes, wire material types, and ability to embed wire on FDM parts built out of different materials. Quantitative results of different experiments are discussed in Chapter 6. The results discussed demonstrate how the mechanical properties are altered when embedding Nickel-Chromium wire onto Polycarbonate (PC) FDM-built parts, results of a continuity test, positional accuracy of the TWE tool, and measuring straightness of 28 AWG embedded lines. Finally, conclusions and recommendations for future work are offered in Chapter 7.

Chapter 2: Literature Review

2.1 INTRODUCTION

Additive manufacturing (AM) is a process with the ability to fabricate three dimensional solid objects of arbitrary shapes from digital models. Other terms used synonymously to refer to additive manufacturing include 3D printing, layer manufacturing, rapid prototyping, layer-wise fabrication, solid freeform fabrication, and direct digital manufacturing (DDM). Much of the initial uses that AM technologies were implemented for were primarily used solely for prototyping. The sustainability of AM technologies today have geared advancements to focus on creating end-use parts in efforts to making a shift to DDM (Chen, *et al.*, 2015.). Several AM technologies exist today and generally they will render eight steps during fabrication of a part which comprise of; 1) creating a CAD model, 2) converting the CAD model into an STL file format, 3) generating toolpaths from the STL file and uploading them onto AM machine, 4) setting up AM machine (calibrating, material loading, etc.), 5) build in a layer-by-layer manner, 6) removing the printed part from the AM machine, 7) post-process part (if necessary), 8) application. AM technologies include Vat Photopolymerization, Powder Bed Fusion, Material Extrusion, Material Jetting, Binder Jetting, Sheet Lamination, and Directed Energy Deposition Processes (ASTM F2792, 2015). With advances in AM technology, the application of AM processes have continued to shift from rapid prototyping to rapid manufacturing of tooling and end-use parts for aerospace, automotive, biomedical, and other applications (Guo, Nannan, and Leu, 2013).

Due to the process taking place in a layer-wise manufacturing process, fabricating one layer at a time, allows access to any layer at any given time. Opportunities arise to improve on functionality of the part because the FDM building process can be interrupted in order to access any individual layer preferred. For example, complementary technologies can be introduced at

various layers to improve the functionality of the final part and develop a multifunctional product. Such complementary technologies include electronics, electromagnetic devices, or mechanical reinforcing type materials. Much research has been conducted over the years to implement these ideas and create end user products (Neotech-AMT 2016.).

2.2 TECHNOLOGIES CONSIDERED FOR ELECTRONIC APPLICATIONS ON FREEFORM SURFACES

Gravure, offset, and pad printing are some methods used to create conductive traces for electronic use and allow a higher conductivity due to the thickness of a pattern that can be applied (Pudas, *et al.*, 2004) (Pudas, *et al.*, 2005). Gravure printing is a printing process which involves a roller with a chemically or mechanically engraved pattern used to transfer ink to press the image onto a substrate. New materials and approaches are a requirement to improve on the printing technique to increase its electronic application (Puetz, Joerg, and Aegerter, 2008). Therefore, much work is required to pursue these mask or screen type of printing as a promising technology to fabricate 3D printed electronics. Direct Write (DW) technologies have been compared to these types of printing and show advantageous features to produce electronic components (Kadara, *et al.*, 2008). Table 2.1 shows a list of printing technologies that are of interest for printed electronics along with their significant characteristics (Sridhar, *et al.* 2011).

Table 2.1 Printing technologies that are of interest for printed electronics along with their significant characteristics

Printing Technologies	Unique Characteristics
Offset Printing	Printed pattern defined by differences in wetting of a plane surface

	Thin layers down to 0.5 μm possible; high resolution (<20 μm)
	Dynamics viscosity of ink: 40 to 100 Pa.s
Gravure Printing	Printed pattern defined by surface relief (recesses) of master
	Broad thickness range (~1 to 8 μm); high resolution (<20 μm)
	Dynamic viscosity of ink: 0.05 to 0.2 Pa.s
Flexographic Printing	Printed pattern defined by surface relief (raised features) of master
	Thin layers of about 1 μm possible; high resolution (~20 μm)
	Dynamic viscosity of ink: 0.05 to 0.5 Pa.s
Screen Printing	Printed pattern defined by openings in printing master
	Thick layers (>10 μm) possible; low resolution (~100 μm)
	Very broad dynamic viscosity range, from gravure inks to offset inks
Inkjet Printing	Master-less; droplet size determined by nozzle diameter and waveform
	Thin layers down to 100 nm possible; moderate resolution (~50 μm)
	Dynamic viscosity of ink: 1 to 20 mPa.s

Direct Write (DW) technologies in its broadest sense can mean any technology which can create two or three dimensional functional structures directly onto flat or conformal surfaces in complex shapes, without tooling or masks. DW technologies in the additive manufacturing community are typically understood as processes which create meso-, micro-, or nanoscale structures using a freeform deposition tool (Gibson, *et al.*, 2015).

Incorporating inkjet printing has also been explored as a DW technology to be used to create organic electronic devices, direct writing of electronics onto flexible substrates, as well as biotechnology and biomedical materials (Calvert, 2001). Many challenges are still being undertaken for these technologies to be enabled to produce end use devices. Much of the most recent work has looked into material (ink) development as well as additional applications that demonstrate the sustainability of inkjet printing for printed electronics (Sridhar, *et al.*, 2011). Although inkjet printing has proven it can have a strategic role in printing electronics when it comes to –micro and nanoscale size layers, there still exists a wide gap between the end use structural, heat resisting, electrical resistance, and functionality for aerosol jetting, micro-dispending, thermal spray, and inkjet printing to be used (Szczech, *et al.*, 2002). The Palo Alto Research Center (PARC) has begun to bridge that gap by developing a "rapid digital manufacturing system" which incorporates inkjet and extrusion based techniques on the same platform as illustrated in Figure 1 (Ready, *et al.*, 2013).

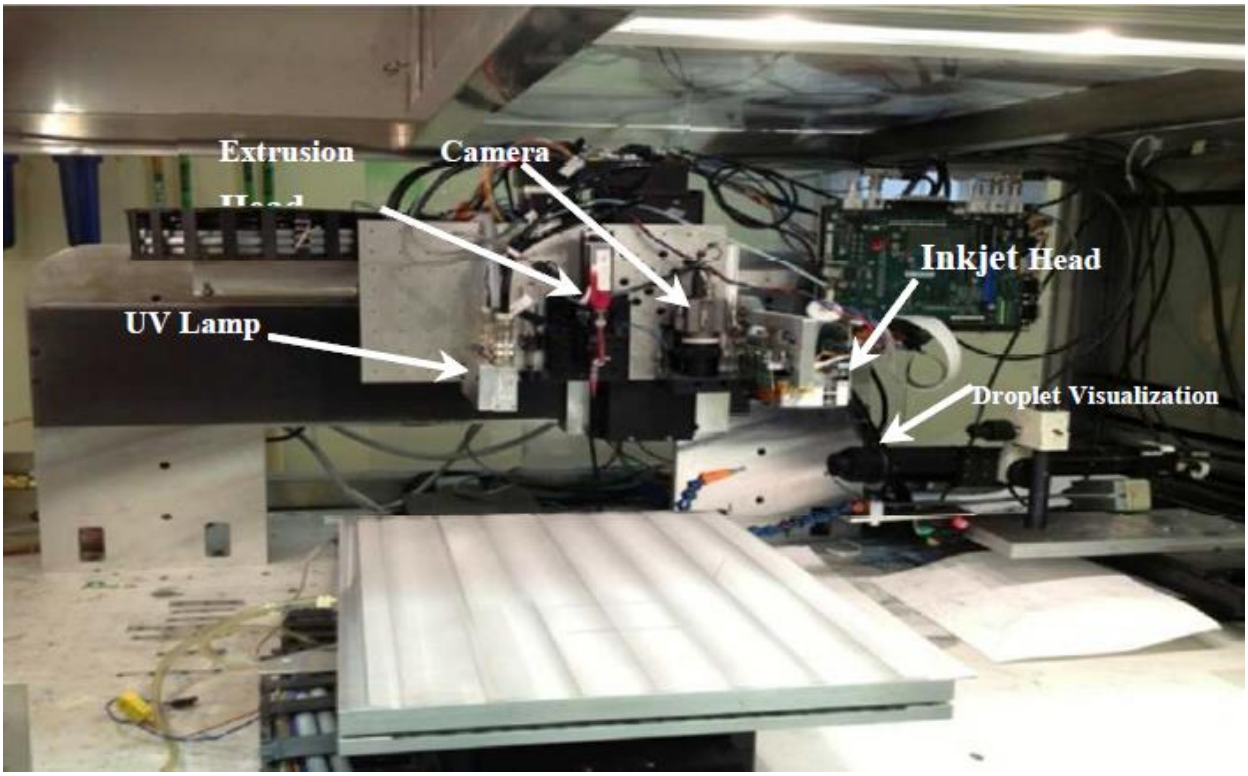

Figure 1 – Initial 3D high accuracy printing system intended to demonstrate 3D multi-functional object fabrication. (Ready, Steven et al. "3D Printed Electronics." NIP & Digital Fabrication Conference. Vol. 2013. Society for Imaging Science and Technology, 2013. 9–12. Google Scholar.)

Conductive inks utilized in the form of micro dispensing has also been explored to create 3D printed parts with electronic and electromagnetic functionality. Micro dispensing is a nozzle DW process which utilize a pump or syringe mechanism to deposit conductive inks through an orifice to form the conductive traces onto a substrate. Ample research has been conducted in this area to develop the automation and possibilities of 3D printed models embedded with electronic components. Stereolithography (SL) has been a widely used AM technology to manufacture highly complex and accurate 3D prototypes due to its high build resolution, accuracy of an SLA-250 is typically quoted as 0.002 in./in. with a surface finish ranging from submicron Ra for upfacing surfaces to over 100 μm Ra for surfaces at slanted angles (Gibson, *et al.*, 2015). In the W. M. Keck Center for 3D Innovations located in The University of Texas at El Paso, a hybrid manufacturing system was developed which integrated SL and micro dispensing in efforts to provide the ability

to fabricate 2D and 3D monolithic structures with embedded electronics and circuitry. The early version of the hybrid system was developed to prove the concept for simple 2D circuits. (Medina, *et al.*, 2005). A wireless motion sensor with GPS navigation was also fabricated using the SL DW ink dispensing hybrid machine to further demonstrate the capabilities of the (SL/DW) tool (Navarrete, *et al.*, 2007). Further advancements were displayed throughout the years and this work can demonstrate broadly what can be achieved by integrating multiple AM technologies and produce 3D monolithic structures with embedded electronics and printed interconnects. (DeNava, *et al.*, 2008) (Navarrete, 2009) (Olivas, 2011) (Gutierrez, *et al.*, 2011) (Lopes, *et al.*, 2012). Within the decades work of developing the methods and systems that led to the recognition of integrating electronics within complex 3D printed parts, research was conducted in efforts to develop multiple material structures which can lead to advance capabilities with mechanical, electrical, and biochemical functionality (Wicker, MacDonald, 2012). Novel ideas of these 3D structural electronics show enhancing 3D printing in a way that will one day ultimately offer unit-level customization and manufacture end-use parts without sacrificing a more intricate structure due to its complexity or time development. A case study showed that a four generation novelty electronic gaming die can expedite prototyping and dramatically reduce the development cycle from weeks, with traditional manufacturing, to hours with 3D printing (Macdonald, *et al.*, 2014). The FDM AM technology has also been utilized with micro dispensing and has resulted with 3D printed antennas also being shown to perform comparably to traditionally fabricated antennas (Deffenbaugh, 2014). With the extensive use of conductive inks, much work is still required to optimize the electrical performance in conductive traces created from micro dispensing. Although increasing the curing temperatures decrease resistivity of the conductive ink (i.e. DuPont CB028, cured for 1 hour at 40 °C measures between 24 mΩ/sq and 47 mΩ/sq vs 16 mΩ/sq cured for 1 hour at 160 °C), the

limitations to intensify the conductivity of conductive traces on these 3D printed electronics are levied by the allowable curing temperatures of the model material used. A novel method, using ohmic heating, has been demonstrated in efforts to decrease the resistivity in conductive traces (Roberson, 2012). Voxel8 has commercially released a 3D electronics printer with a desktop FDM printer model and integrating micro dispensing technology with conductive silver ink. Voxel8 has been able to successfully print a quadcopter with human involvement required to add parts. ("Voxel8: 3D Electronics Printing."). A push to develop higher power electronics has required a more conductive trace and heat resistant material for the aid in the evolution of 3D printed electronics. FDM and solid conductive wire have been explored to fulfil these needs.

2.3 FUSED DEPOSITION MODELING

Fused deposition modeling (FDM) is an extrusion-based AM technology which is currently the most popular AM technology on the market ("Wohlers Talk" Popularity of FDM). Due to the popularity of FDM technologies, subsequently much research has been performed to innovate on the applications of FDM-printed parts, discussed in the latter. FDM machines made by Stratasys, Inc. are very successful and meet the demands of many industrial users, partly due to the material properties and the low cost of the entry-level machines (Gibson, *et al.*, 2015).

The materials in FDM technologies are fed in a continuous solid filament and into the system. Once in the system the solid filament is pushed through a heated chamber, referred as the liquefier, which softens the thermoplastic. The thermoplastic is driven by pinch rollers which generate enough pressure to extrude the semi-molten plastic out through a nozzle. The nozzle traverses along its designated toolpaths in order to extrude the model material or support material. The support material is one of the reasons why it is possible for the complex features to be created.

This material can easily be broken off or removed in an ultrasonic bath. Once the nozzle has concluded its toolpaths in one layer, the build platform descends in the Z direction and allows for the next layer to be build adjacent to the previous layer. There exists a large variety of materials which can be used on FDM machines, Table 2.2 features a list of some commercially available FDM materials along with some of their respected material properties (Hossain, 2014).

Table 2.2 Material Properties of commercially available FDM materials

Material Property	ABS	PC	PC-ABS	ULTEM 9085	PPSF
Tensile Strength (MPa)	22	68	41	71.6	55
Tensile Modulus (MPa)	1627	2300	1900	2200	2100
Elongation (%)	6	5	6	6	3
Glass Transition Temperature (˚C)	104	161	125	189	230
Specific Gravity	1.05	1.20	1.10	1.34	1.28
Thermal Expansion (mm/mm/˚C)	$10.08*10^{-5}$	$6.84*10^{-5}$	$7.38*10^{-5}$	$6.6*10^{-5}$	$5.5*10^{-5}$

2.4 EMBEDDING COMPONENTS ON FDM-PRINTED MODELS

A significant objective in the AM industry is to produce end-use parts. With the ability to create complex geometries, FDM-printed parts alone produce a relatively low cost structurally functional model. Earlier research demonstrated the idea of embedding components, which

allowed a higher level of application, such as fabricating robotic limbs with embedded sensors and actuators, to this manufacturing process (Bailey, *et al.,* 2000). Employing the ability to add electronic elements to these models will result in evolving the functionality of an FDM-printed part. Through strategic design, high power electromechanical applications can also be enabled to some of these relatively inexpensive printers. A 3D printed motor is demonstrated, showing that additive manufacturing is comparable to a traditionally fabricated commercial motor. This work involves much human interaction to be completed but it broadened and demonstrated more applications for FDM manufactured parts (Ramos-Almeida, 2013) (Aguilera, *et al.*, 2013). The goal to reach a fully automated FDM system with integrated technologies is a significant growth to the AM industry which will allow the shift to DDM and endless conceptualization of what and where FDM-printed instruments can be applied to. The development of the Multi^{3D} system displays how integrated technologies can be integrated to enhance the capabilities of a part being built. Much research has been conducted to develop and demonstrate the ability of fabricating a part with multiple materials using multiple FDM technologies, this would otherwise be impossible to fabricate with traditional means such as injection molding (Espalin, 2012). Adapting complimentary technologies to the multi-material, multi-technology (MMMT) FDM system such as, micromachining, component placement, ink dispensing, and embedding of wire allows the shift to DDM to be progressively achievable. Motivation for embedding conductive metal wires has been explored to outperform what conductive inks are limited too. As previously discussed, conductive inks are limited in terms of reliability and performance due to requiring higher curing temperatures to aid in reducing their resistivity. From an applications standpoint, Table 2.3 compares the resistivity and resistance values independent of geometry between commonly used conductive inks, extruded solder, copper wires, and traditional PCB manufacturing values at 10

cm of length (Espalin, *et al.*, 2014). The bare solid copper wire proves to be a material of interest for the use in 3D printed electronics due to its low resistance values. As previously discussed much research has been focused on using inks to create 3D printed electronics and therefore results in much research lacking the utilization of copper wire for these application. One method developed in the W.M. Keck Center at UTEP to embed the copper wire consisted of an ultrasonic horn, modified to allow a wire to be fed perpendicular to the plane of interest. Another process in development in the W.M. Keck Center at UTEP is a joule heating method which heats the wire by passing electrical current and subsequently is able to be submerged into the substrate (Espalin, *et al.*, 2014).

Table 2.3 Comparison of resistivity and resistance for select conductors

Case	Geometry	Resistivity (Ω*m)	Resistance (Ω)
1 oz. copper PCB with 4 mil width	37 µm thick, 100 µm wide, conductor 10 cm long	$1.7*10^{-8}$	0.45
DuPont Ink CB028 Silver	25 µm thick, 100 µm wide, conductor 10 cm long	$11.8*10^{-8}$	4.73
DuPont Ink CB500 Copper	25 µm thick, 100 µm wide, conductor 10 cm long	$50.7*10^{-8}$	20.27
Extruded solder	25 µm thick, 100 µm wide, conductor 10 cm long	$7.2*10^{-8}$	2.86
40 gauge copper wire	80 µm diameter, conductor 10 cm long	$1.7*10^{-8}$	0.33
32 gauge copper wire	200 µm diameter, conductor 10 cm long	$1.7*10^{-8}$	0.05

28 gauge copper wire	320 μm diameter, conductor 10 cm long	$1.7*10^{-8}$	0.02

Although the methods previously mentioned to embed conductive wire have shown potential, they also have their drawbacks. The ultrasonic processor is a relatively expensive piece of equipment and can cost as much as a high end 3D desktop printer. The ultrasonic embedding process is also a very unforgiving process where a slight offset between the horn and substrate can cause the wire to shear. Another drawback of the ultrasonic horn is that it can damage components placed on the printed model due to the localized high frequency vibrations. The joule heating method on the other hand provides a more forgiving process with a less abrasive embedding procedure. A disadvantage that the joule heating method inherits is that it required multiple degrees of freedom in order to achieve turns in the wire pattern. Another direct wire embedding technology has been found which uses a heating element to heat plastic external to the tip as well as the wire inside the tip. This basic design of embedding wire is similar to the research conducted in this thesis and also displays great potential to embedding conductive traces. The obstacles faced during their development of the concept was the ability to find a solution to perform a successful cutting operation as well as develop a method to fully embed and accurately submerge a wire in a surface without the aid of cavity-like guides (Bayless, *et al.*, 2010).

Chapter 3: Development of the Thermal Wire Embedding Apparatus for FDM-Printed Parts

3.1 Thermal Wire Embedding Prototype

In this work the concept of a thermal wire embedding (TWE) apparatus was proposed. The TWE device entails of a technology that will be used to deposit metal wire in a specified pattern on a specified layer(s). The TWE technology will be able to traverse perpendicular to a surface or interlayer(s) of interest of an FDM-printed part. The wire pattern can potentially be used for any electronic application found that can utilize the wires electrical properties. Another application for the wire pattern is as a mechanical property supplement, which was approached with the thought of it being analogous to how carbon fiber can be used to reinforce polymers. The following sections will describe how the TWE prototype tooling was developed.

3.2 Thermal Wire Embedding Mechanism

The TWE technology was developed to consist of a thermally heated block for housing two cartridge heaters which provide direct heat conduction throughout the heated block. The heated block also houses a metal tip that features an internal channel which is used to guide wire through it and exit out of its orifice. The orifice is perpendicular to the surface of the substrate or interlayer of interest in which the TWE technology will be embedding the wire pattern onto. Another feature of the heated block is an internal channel that allows a hypodermic tube to be inserted into and continue throughout to connect the channel to the opposing side where the embedding tip is attached to. The hypodermic tube is used as a guide for the wire to be fed through the inside of the hypodermic tube, directing it through the internal channel within the heated block, following the embedding tips channel, and exiting out of the orifice of the tip. Using the hypodermic tube as a guide outside of the thermally heated enclosure is beneficial when feeding wire from a spool of coiled wire and it is required to reintroduce wire. The hypodermic tube also allows the wire to straighten its profile before it reaches the internal cavities of the heated block and wire embedding tip. The hypodermic tube also gives the operator a distance that is at a lower

temperature away from the heated block when needing to feed wire manually once the block has reached the high temperature levels required to thermally embed wire. The Proportional Integral Derivative (PID) controller is often used in industries because of its simplicity and wide range of applicability such as temperature controllers used for industrial ovens, plastic injection machinery and hot stamping machines. A PID controller is designed for various forms of integrating systems with time delay using direct synthesis method (Anil, 2015). The temperature levels were controlled through a PID temperature controller which allowed to measure and control the temperature settings for the TWE tool. Given the known properties of the materials used to extrude with the FDM technology, such as the glass transition temperatures of these thermoplastics (Table 2.2). The information known of these thermoplastics was a great start for the temperature settings on the PID temperature controller in order to begin the wire embedding process. Research was conducted to determine the temperature settings for the different thermoplastics that would be used. The research not only included experimenting with different temperatures for the diverse thermoplastics used but the traverse speed settings when embedding a metal wire pattern. The goal to reach for the final parameter settings was first established to be able to successfully embed straight lines on a substrate and progress from there. This simple design allowed us to test the concept of being able to embed metal wire onto a FDM-printed substrate.

3.3 THERMAL WIRE EMBEDDING COMPONENT DETAILS

The TWE tool was composed of an OMRON E5CN PID temperature controller with a type k thermocouple, an insulation enclosed with machined heating block which houses two 100 W cartridge heaters, a machined metal tip, a hypodermic tube, and an air slide with two parallel guide rods. The heating block (Figure 2) was machined, in-house, out of 6061 aluminum due to its good machinability, good structural properties, and another property; which is essential to achieve a reasonably quick thermal distribution, is that aluminum 6061 is a good heat conductor. The

cartridge heaters used were two 100W powered single phase, magnesium oxide encased in a type 304 stainless steel sheath, hardwired leads, which can withstand maximum temperatures of just over 500 ˚C. The metal tip was also machined internally out of aluminum in order to achieve as much of the thermal conduction to transfer to the tip and the metal wire while embedding. The hypodermic tube used was made out of type 316 stainless steel, which is a common material for hypodermic equipment due to its strength and resistance to corrosion.

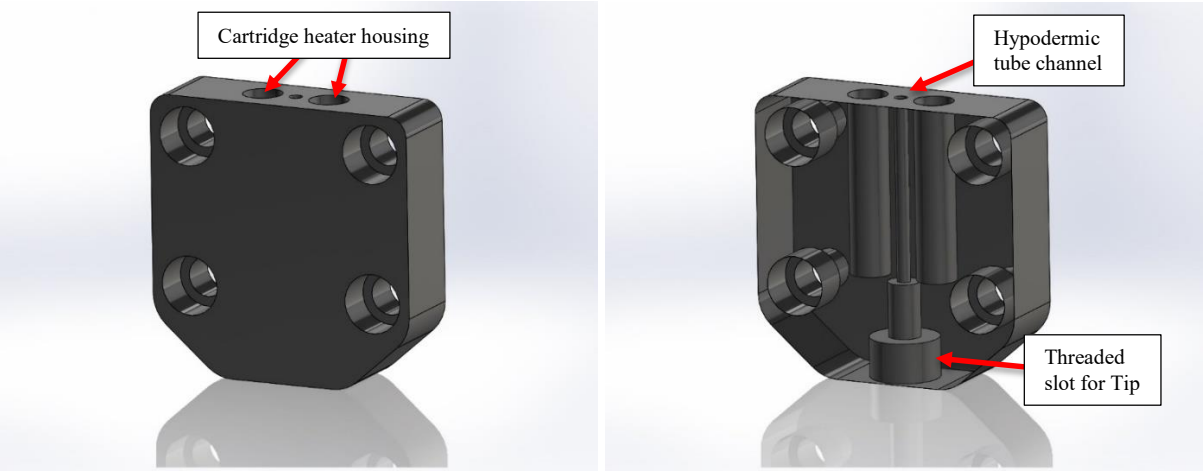

Figure 2 – CAD of Solid heated block (left) and a transparent heated block (right)

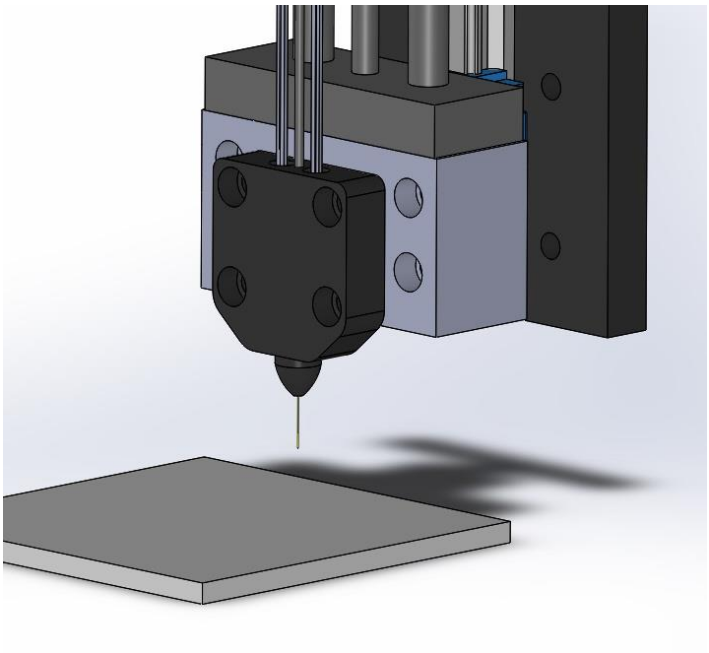

Figure 3 – Concept TWE apparatus

3.4 THERMAL WIRE EMBEDDING APPARATUS ASSEMBLY

A CAD assembly of the TWE apparatus can be seen in Figure 3. Fabricating the heated block involved drilling two holes to sit the cartridge heaters in, a bore to tap and thread the aluminum tip as well as a counter bore for the tip to secure in, 4 holes with counter bores to mount the heated block with bolts, the final feature in the heated block consist of drilling the internal channel for the hypodermic tube, this can be seen in Figure 2. The tip features a drilled hole for the internal channel which was used for the metal wire to enter as well as exit out of the opposing orifice. The tip also was machined with a boss which was used to create the external thread that mates with the internal thread on the heated block. The enclosure used to surround the mineral wool, which was used to insulate the tool head, was made out of sheet metal and bent to contour the shape of the heated block and mineral wool. Kapton polyimide tape, a DuPont silicon adhesive film that withstands a wide range of low and high temperatures, was used to aid and seal the sheet metal enclosure from unclasping (http://www.kaptontape.com/1_Mil_Kapton_Tapes_Datasheet.php). The TWE tool used a ball-bearing carriage attached to an air slide that allows a steady motion when extending or retracting the tool. The air-slide and carriage were not fundamental components to the TWE tool, but they were added as an option because the TWE apparatus was considered to be used next to other tooling heads on a separate system in the future as shown in Figure 4 (Ambriz, 2015) (Coronel, 2015). With the addition of the air-slide and carriage, incorporating a convective cooling hose to be placed between the heated block and the fixture was required; in efforts to moderate the amount of heat conducting to the rest of the system. Other fixtures machined were to mount the TWE tool onto the 3 axis gantry used. These fixtures can change depending on the gantry or framework the TWE tool is being installed on. The TWE head was installed on an Aerotech XYZ gantry system. As most motion control systems, G-code was used to coordinate and position the TWE head in the X-, Y-, and Z-directions. The installation of the TWE apparatus is shown in Figure 5.

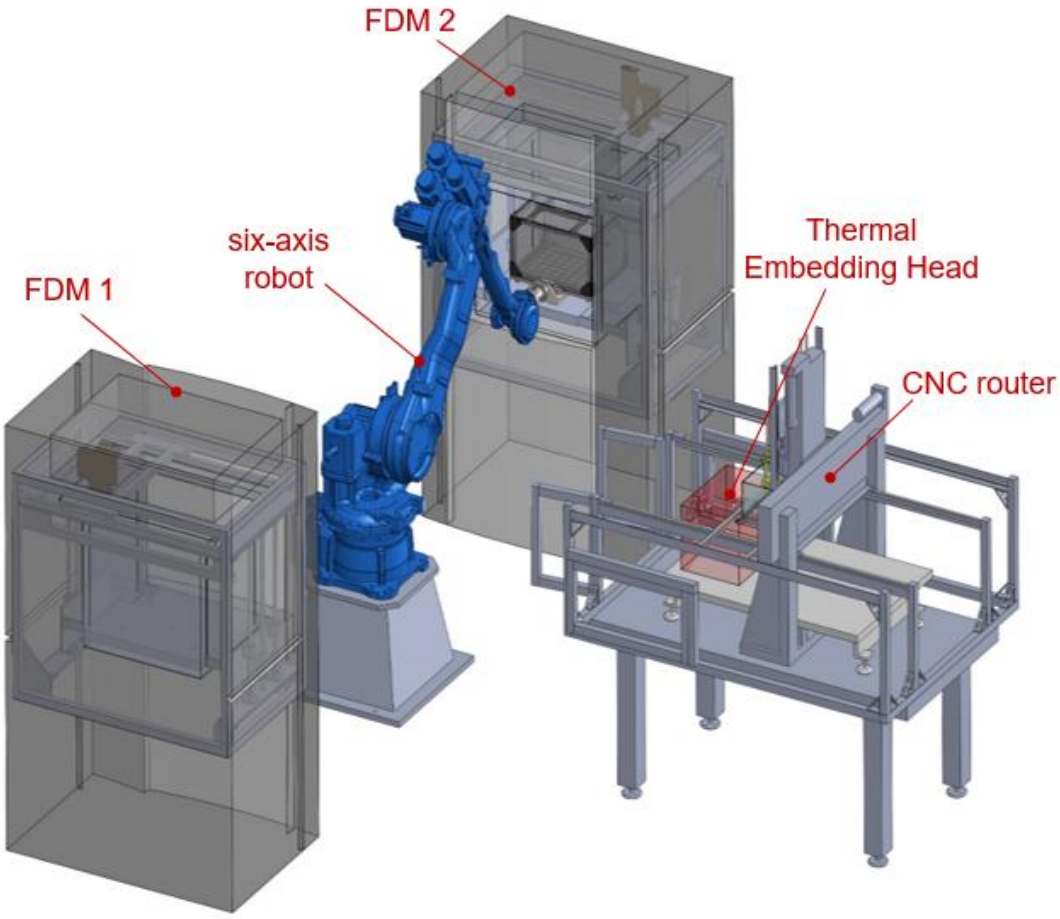

Figure 4 – Multi^{3D} System (Ambriz, 2015) (Coronel, 2015)

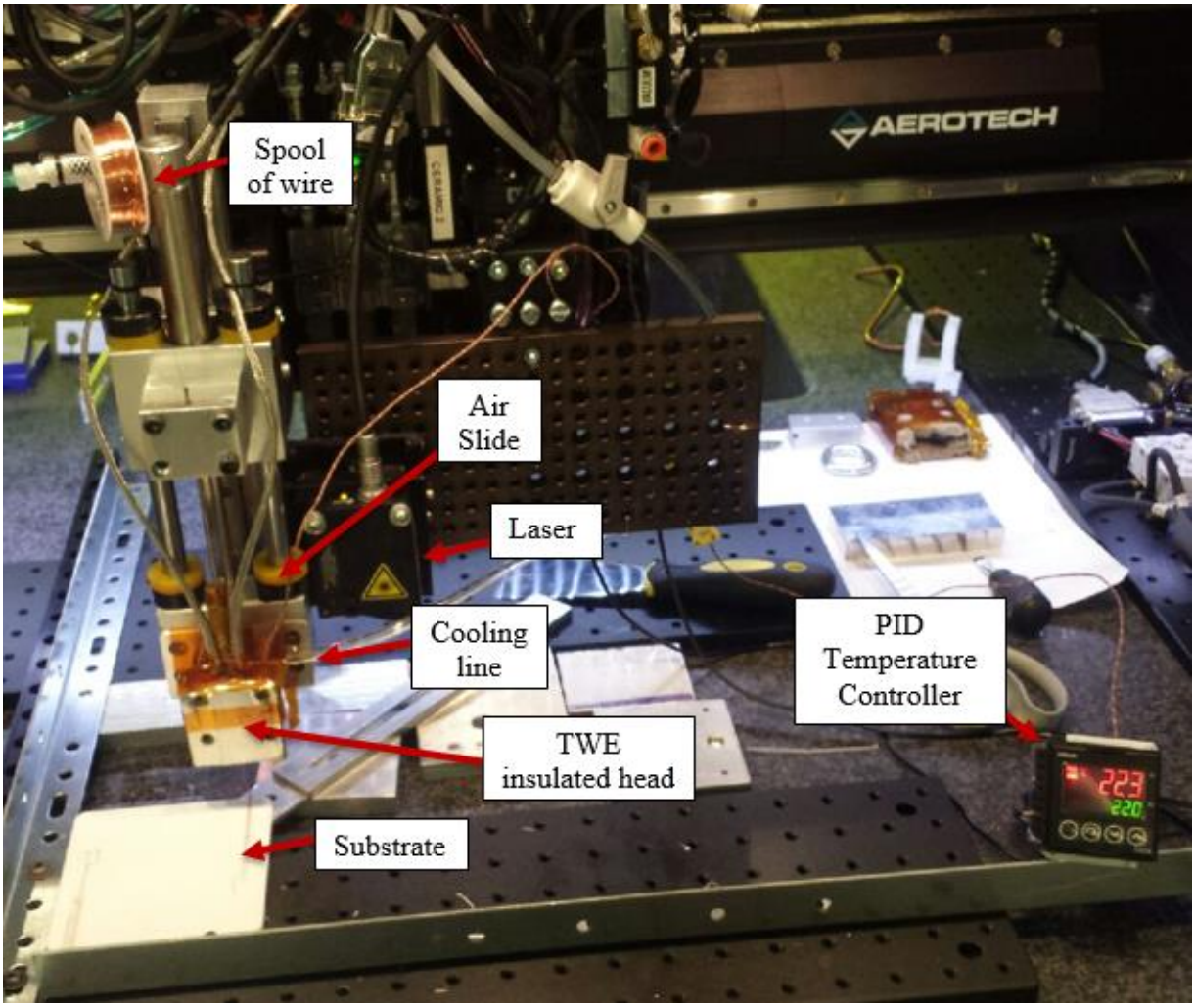

Figure 5 – TWE installed on an Aerotech Gantry

3.5 PARAMETER DEVELOPMENT FOR THE THERMAL WIRE EMBEDDING TOOL

Conceptually, the idea to begin wire embedding with the TWE tool was to set the temperature controller to a temperature set-point value above the thermoplastic's respective glass transition temperature. The glass transition temperature baseline was thought appropriate for this process because in order to embed wire into the layer, the material must be soft enough to allow penetration and encapsulate the wire. The primary focus was on polycarbonate (PC) substrates to be the material choice for the first experimental trials of 32 American Wire Gauge (AWG)

copper wire. This gauge of wire is equivalent to 202μm or 0.00795in. Based on the supplier's specifications, the copper wire meets the ASTM B3 standards (relevant properties shown in Table 3.1) and has a tensile strength of 29 MPa (http://www.mcmaster.com/#standard-copper-wire/=10s1zoi). The traverse speeds were determined that they can vary during the experimental steps but were strategically chosen so that the embedding process would not move slower than 1 mm/s. The speed constraint resulted with several trial and error experiments to determine a TWE tool temperature. As shown in Figure 5, custom fixtures on an optical breadboard were used to secure the substrates into position. Before initiating the wire embedding process, it was required to register the parts position with the machine's global operating coordinates. The programming method used was absolute Cartesian coordinates with G54 work offsets (Xun, 2009). Registering the zero point on a work piece varied and was dependent on the embedding toolpaths designed. The registration procedure was subject to change based on the wire embedding strategy.

Table 3.1 Relevant properties required for standard (ASTM B3) of copper wire

ASTM B3 Standards
Density 8.89 g/cm^3 (0.32117 lb/in.^{3}) at 20°C
15% Elongation in 10 in during tensile testing
Electrical resistance: not exceed 0.15328 Ω·g/m^2 (875.20 Ω·lb/mile^2) at 20°C
Permissible wire variation: no more than plus and minus 0.0025 mm (0.0001 in.)

3.6 THERMAL WIRE EMBEDDING METHODOLOGY

As the TWE tool approached the substrate, the tip began to radiate heat onto the surface. Wire embedding only occurred after the tip came into contact with the surface and conducted enough heat to soften the surface. It was observed that the heated metal wire itself can generate enough heat and embed itself if the wire is directed to the substrate to penetrate the surface. The heated wire can initially embed itself but as the tool traverses, it will not continue to embed itself throughout a toolpath due to how soft the material is. The wire can easily be pulled out of the soft material when the TWE tool traverses. It was found that the TWE process can be achieved once the heated metal wire became sandwiched between the tool's heated tip and the surface of the substrate. In order to initiate the wire embedding process, with the prototype TWE tool, the heated wire was required to have enough of a lead which allowed the operator to clamp onto the wire with needle-nose pliers. Gripping the free lead of the heated wire was required to balance the pull forces applied to the wire while the tool traversed on the substrate. While gripping the free lead, the remainder of the wire would "self-feed". "Self-feeding" occurs when the metal wire outside of the tool's tip is fixed and while the tool traverses along a toolpath, as long as the wire does not shear, it will continue to "self-feed". "Self-feeding" occurs due to the tension that is created within the metal wire and subsequently rotates the spool of wire to continue feeding the wire.

A detailed description of the wire embedding process is provided here as well as observations during the process. Note that this description applies only to the prototype tool. The second and third tool described later in the document have different operations and yielded different results. To initiate the wire embedding process, it was required to grip the lead of wire with pliers and position the pliers planar to the surface so that the wire that is gripped, is resting on the surface of the substrate once the tool comes into contact with the surface. As the tool is about to embed, it is important to note that the operator is required to hold onto the wire in the opposing direction of the path of travel. With the tool initiating contact with the surface, the tool continues to traverse over the substrate inducing the plastic to soften while the wire self-feeds.

After the tool leaves a region, the softened material hardens and encapsulates the wire. Once the material in the initial procedure hardens, with the embedded wire, the operator can then release the grip of what is now the tail end of the embedded wire. The solid material, encapsulated with the deposited wire, can now withstand the tension required to continue embedding and rotate the spool of wire and "self-feed". It was observed that the tool height offset played an important role in order to successfully embed wire. Improper height offsets resulted in 1) the wire slipping on the substrate's surface without becoming encapsulated when the height was too large and resulted in marring the plastic surface, or 2) the wire breaking on the surface if the height was too low.

3.7 TOOL HEIGHT OFFSET

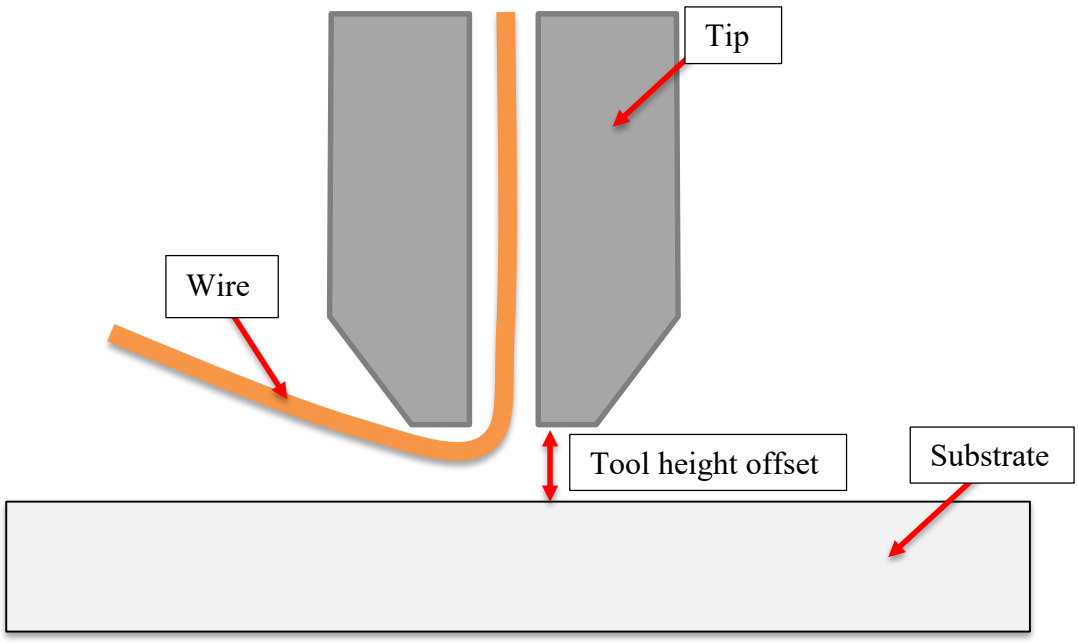

Figure 6 – Diagram of tool height offset

The offset registration with the tool is an important step of the TWE process. The offset from the surface of the substrate was measured with a metric feeler gauge. The feeler gauge consists of multiple thin blades that are calibrated to a known thickness which assisted in measuring the narrow gap between the thermal embedding tool tip and the substrate's surface. The

feeler gauge allowed to experiment with the offset distance, displayed in Figure 6, to ascend or descend the tool's tip to the plastic surface. These experiments, described with more detail in Table 3.2, resulted from wire not being able to embed, another result was partially embedding a wire, as well as embedding a wire with minimum heat affected zones, and embedding a wire with relatively large heat effected zones around the embedded wire as shown in Figure 7. Results also varied in the head and tail end of a trace due to the human involvement during the beginning and conclusion of a wire embedding process. The human involvement can lead to accidentally pulling the wire out of its position or potential damage to the wire or substrate.

Table 3.2 Qualitative results of tool height experiments

Results	Comments
Wire not embedded	This is due to the tool height offset being too large
Partially embedded wire	Tool height offset to part is not consistent. Part might not be leveled. Wire might have sheared
Wire embedded with minimal heat affected zones	Tool height is properly calibrated
Wire embedded with relatively large heat affected zones	Tool is too far into the FDM-printed part

The offset registration for the set up also involved registering the X- and Y- axis. The axis registration points are dependent on the origin of the toolpaths and the placement of the designed traces relative to the part. The method used to register these points were with the aid of a camera and a digital video image generator (DCG – 200M). Using the camera and DCG tool required to fix the camera onto the gantry and measure the offset between the camera and TWE tool in the X- and Y- axis. Knowing the offset between the camera and the TWE tool enabled the placement of the TWE tool over the camera's target.

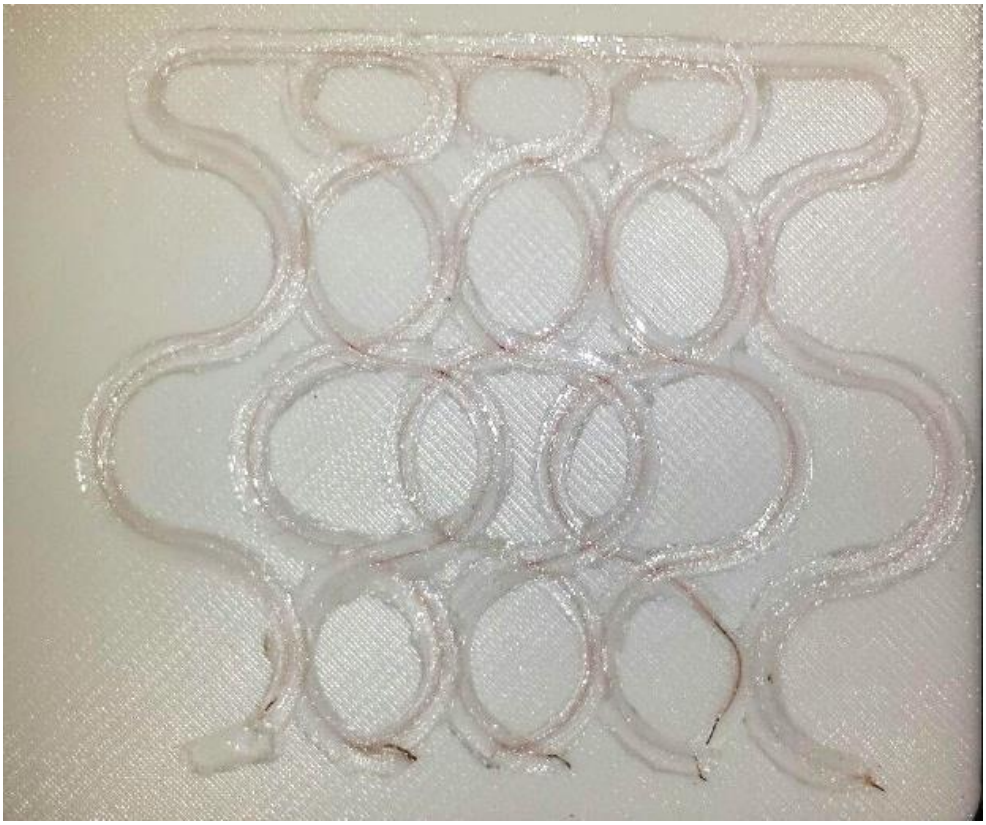

Figure 7 – 32 gauge copper wire with large heat affected zones

Figure 8 – 32 AWG embedded copper wire in PC

3.8 PARAMETER EVOLUTION

The encouragement of being able to embed straight lines, demonstrated in Figure 8, with repeatable results lead to attempting to find a method to introduce turns in the wire pattern. The challenge with the turns was having to simulate the effects the operator has when gripping the lead of the wire in the initial embedding process. This was a challenge because as the tool changes directions to create a corner, the small area on that corner does not have enough strength to balance the tension required to hold and "self-feed" to the adjacent direction. This is a result of the material at that point, on the corner, being too soft that it does not provide the "self-feed" mechanism the TWE tool requires for the wire embedding to continue. Many attempts lead to the wire being pulled out of its track and continue being pulled out of its track. It was also observed that the tension could be reintroduced to continue to "self-feed" after a failed corner turn as shown on the image to the right in Figure 9. The image to the left in Figure 9 illustrates the intended wire pattern design and highlights some points referring to the image on the right. Point 1 highlights the start of the pattern, point 2 notes that the turn was successfully embedded on the actual embedded wire pattern, point 3 notes that the turn was unsuccessful and the wire was pulled out of its intentional position, point 4 highlights that the tension was reintroduced and thus allowing the embedding to continue, points 5 and 6 note the same results as points 3 and 4, finally point 7 highlights the end of the wire pattern.

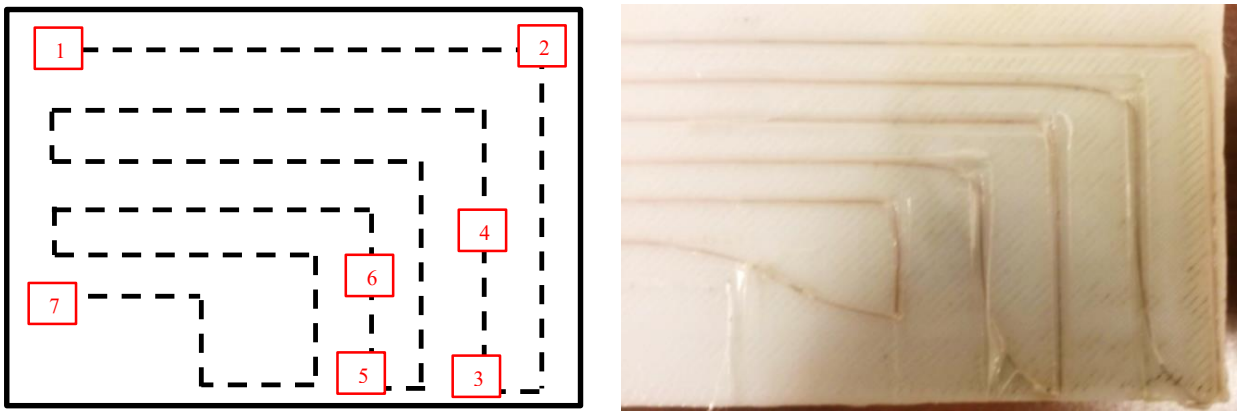

Figure 9 – Design of intended wire pattern (left). 32 AWG copper wire on PC substrate (right). Note the corner patterns are defected due to embedding wire with unmodified G-code.

In order to create the turns, clever G-code manipulation had to be performed. This was done by introducing 2 extra mm in the direction prior to the turn. Once the tool had traveled the extra 2 mms, the tool is commanded to ascend off the substrate, the time off the substrate also allowed the plastic to harden and secure the wire. Once ascended off the substrate, the tool then hovers back to the original destinations point, descend, and proceed to the adjacent direction to achieve the corner turn. With G-code manipulation, we noticed that intricate wire patterns could be achieved as shown in Figure 11. Figure 13 shows a complex wire pattern design. Due to the manual manipulation of the G-code, the time required to finish the full wire pattern shown would require numerous hours to achieve.

3.9 G-CODE

To introduce the toolpaths for a particular wire pattern on a computerized numerical control (CNC) gantry, the G-code language was used to instruct the machine's tool where to move. If the pattern is simple enough to write the G-code manually it is preferred to do so for brevity, i.e. a straight line or a straight line with a turn or two. The method used for a more complex wire pattern was to utilize a computer aided design (CAD) software and produce a wire pattern by creating a

sketch drawing of the pattern with lines and/or curves. Once the complex wire pattern was created, saving it as a DXF file was necessary to generate the G-code. DXF2GCODE is a software tool for converting 2D (dxf, pdf, ps) drawings to CNC machine compatible G-code ("dxf2gcode Download | SourceForge.net."). This software was utilized to convert the DXF file of the wire pattern(s) into the G-code language used on the motion control system. The G-code generated from the DXF2GCODE software included the toolpath for the pattern(s) converted from the DXF file but the G-code is still not ready for use with the wire embedding process. The wire embedding process still required intermittent steps throughout the process in order to initiate the embedding of wire, turning corners, and terminating a wire trace. Thus, it was still required to manually introduce modifications in the G-code language generated from the DXF2GCODE software. These manual modifications were required in order to include the steps found successful during the experimental trials. The overall set up to begin the wire embedding process is shown in Figure 10. The following shows an example of what is generated with the DXF2GCODE software and the commands required to be inserted and modified.

Required Command Modifications:

* Replace any G0 with G1
* Include bottom 3 lines to be the first set of commands in G-code file

    G54 (#) X (#) Y (#) Z //This is your registration point

    G1 X 0.00 Y 0.00 Z 10.00 F10 //This line commands the tool to go 10 mm above the datum

    dwell2 //This command pauses for 2 seconds (allows time to verify registration position)

* After any line with a G1 Z 2.000 insert a dwell4
* After the command line (except for the first) G1 Z 0.000 include a dwell2 //This allows the material of the substrate to soften at the initial embedding stake

* After last Z 2.000 command, insert

dwell4

G1 Z 10.000 F4

dwell6

G1 Z 60.000 F10

(Example) For a 90 degree turn, add 2mm in the direction past the point of a turn

If the command lines generated in DXF2GCODE software are (to embed a 10x10 mm square):

G1 X 0.000 Y 0.000

G1 X 10.000 Y 0.000

G1 X 10.000 Y 10.000

G1 X 0.000 Y 10.000

G1 X 0.000 Y 0.000

After modifying, commands should include:

G1 Z 0.000

dwell2

G1 X 0.000 Y 0.000 F1

dwell2

G1 X 12.000 Y 0.000

dwell2

G1 Z 2.000 X 10.000 Y 0.000

dwell4

G1 Z 0.000

dwell1

G1 X 10.000 Y 12.000

dwell2

G1 Z 2.000 X 10.000 Y 10.000

dwell4

G1 Z 0.000

dwell1

G1 X -2.000 Y 10.000

dwell2

G1 Z 2.000 X 0.000 Y 10.000

dwell4

G1 Z 0.000

dwell1

G1 X 0.000 Y -2.000

dwell2

G1 Z 2.000 X 0.000 Y 0.000

dwell4

G1 Z 10.000 F4

dwell6

G1 Z 60.000 F10

(Example) For 45 degree angles, continue 1mm past the direction of turn

If the command lines generated in DXF2GCODE software are:

G1 X 0.000 Y 0.000

G1 X 10.000 Y 10.000

G1 X 0.000 Y 20.000

G1 X 10.000 Y 30.00

After modifying, commands should include:

G1 Z 0.000

dwell2

G1 X 0.000 Y 0.000 F1

dwell2

G1 X 11.000 Y 11.000

dwell2

G1 Z 2.000 X 10.000 Y 0.000

dwell4

G1 Z 0.00

dwell1

G1 X -1.000 Y 21.000

dwell2

G1 Z 2.000 X 0.000 Y 20.000

dwell4

G1 Z 0.000

dwell1

G1 X 11.000 Y 31.000

dwell2

G1 Z 2.000 X 10.000 Y 30.000

dwell4

G1 Z 10.000 F4

dwell6

G1 Z 60.000 F10

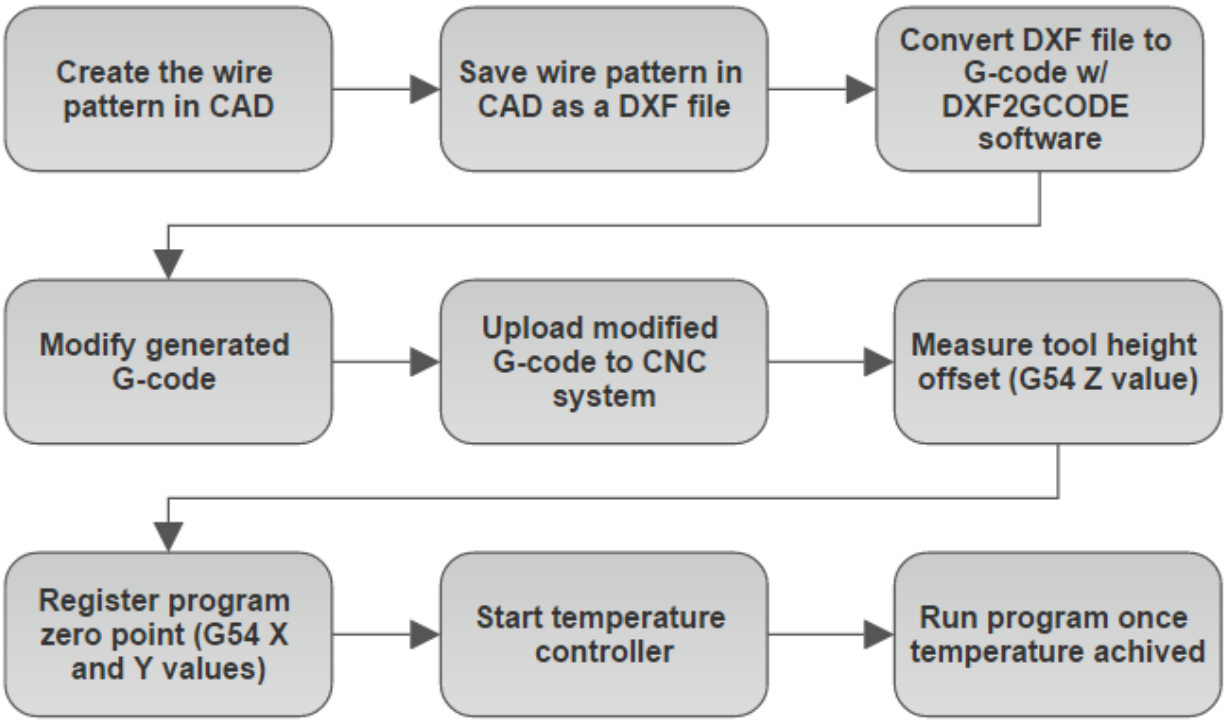

Figure 10 – TWE Process Flowchart

Using the prototype TWE tool, Figures 11 and 12 show some examples of 100 X 100 mm polycarbonate (PC) substrates embedded with 32 gauge copper wire in various patterns. Figure 13 demonstrates a sketch of a complex wire pattern designed and an image of an attempt of embedding the traces shown in the sketch. Due to the intense G-code modifications required, only a partial pattern of the complex design was embedded. This shows the limitations of the process to go from CAD to wire embedding. Also, limitations are seen with the prototype TWE tool due to the human involvement.

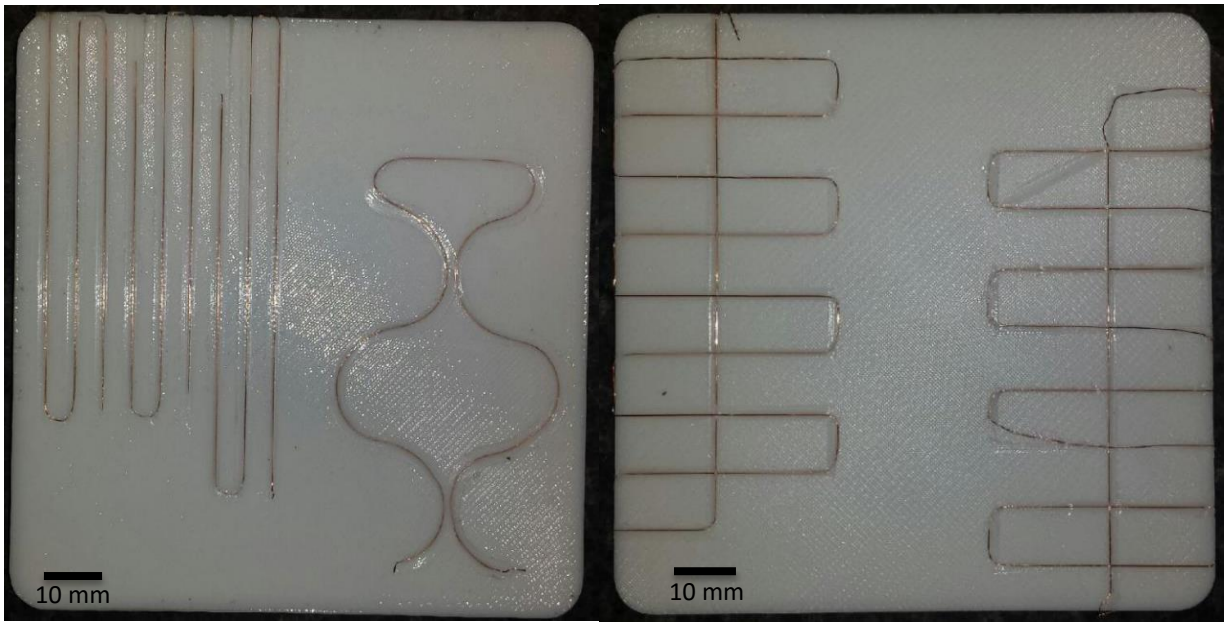

Figure 11 – Embedded 32 gauge copper wires in multifaceted patterns on 100 x 100 mm PC substrates

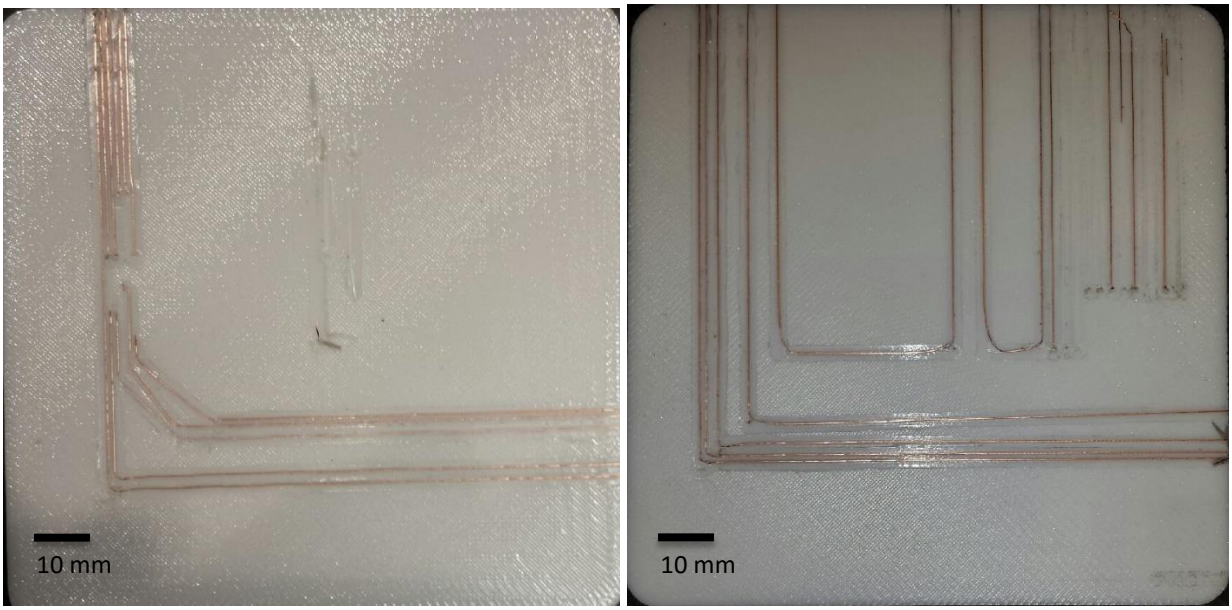

Figure 12 – Embedded 32 gauge copper wires in multifaceted patterns on 100 x 100 mm PC substrates

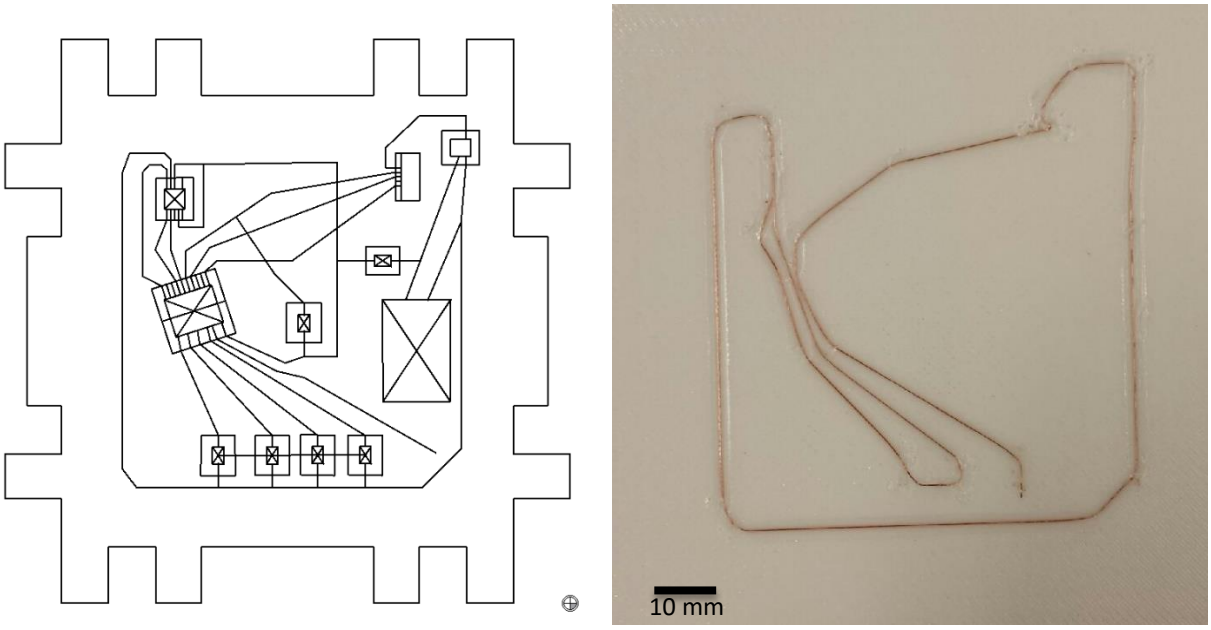

Figure 13 – Sketch of a complex wire pattern (left) and a partial embedded pattern 32 gauge copper wire on 100 x 100 mm PC substrate (right)

Chapter 4: Design development of the Thermal Wire Embedding apparatus for FDM-Printed Parts

4.1 The Second Thermal Wire Embedding Apparatus

Once the TWE prototype proved that wire of different metals and gauge can be embedded onto the various thermoplastic materials that the FDM AM technology can deposit, we were able to further evolve the technology to reach a more fully automated process. With the prototype TWE tool, many limits were reached because of the human involvement required to process a wire pattern onto an FDM printed part. While experimenting with the prototype tooling, we were able to identify requirements to further evolve the technology and reach a more fully automated state. The identified requirements were that a motor was essential to drive the wire for several reasons. Driver feeding the metal wire creates the ability of being able to include a lead of wire of a predetermined length. The driver allows the wire to be re-fed in the instance that a wire is intentionally or unintentionally sheared off. Unintentional shearing could be caused by improper calibration issues with tool height offsets. The motor driver also reduces the internal stresses on the wire that are created when embedding using the "self-feeding" method, which caused friction between the tip and substrate. The friction introduced when "self-feeding" is reduced by driving the wire at the corresponding speed that the TWE tool is traversing throughout its toolpath. A convective cooling tube was also added to locally harden the substrate and cool the wire, which was intended to mitigate the wire slipping observed. The addition of a cutting mechanism also removes the human involvement required to 1) shear the wire at the end of a toolpath, 2) during the initial stages of the wire embedding process, and/or 3) when embedding a new track throughout the designed toolpath. The accuracy of the length of a single wire trace increases by utilizing a cutting mechanism. The accuracy increases as the calibration improves between the predetermined lengths designed for a trace of wire and the cutting mechanism's position. The required maximum shear force to perform the cut on the wire of any material and size can simply be calculated with the wires diameter as well as the materials corresponding ultimate shear strength. The wire will

fail and separate at the cut location do to the applied shearing force exceeding the materials ultimate shear strength.

$$\tau = \frac{F}{A_c}$$

The second TWE tool (concept drawing shown in Figure 14) integrated the components required to remove the human element involved when initiating and concluding a wire pattern as well as give further control of the apparatus. The design introduced two DC motors. One motor, called the spool motor, to rotate the spool of wire which will work in concert with another DC motor, the driving motor, which will drive the wire feeding mechanism. The wire feeding mechanism includes a wheel with shallow teeth which was used to drive the wire. This wheel is coincident on the wire driving DC motor's shaft. The wire feeding mechanism also includes an idler roller which is used to pinch the wire against the wheel with shallow teeth and allowed the wire to drive. This idler roller was attached to a fixture which was displaced with a screw in order to calibrate the tensioning force required to pinch the wire and allowed for the wire to be fed. The idler roller turned on ball bearings to roll with negligible friction and also featured a machined groove, machined with a v-groove lathe cutter, which was used to keep the wire from slipping off of the wire feeding mechanism. The addition of the cutting mechanism included custom fixtures, machined in-house, for the key elements required for the cutting mechanism to operate successfully. Those elements required an electric push actuator that provided force to a machined "T" shaped component which pivoted and swung the attached cutting blade to perform the cut. Heat was conducted to the mounting block through the bolts and spacers used to attach and separate, respectively, the heating block with the mounting block. Therefore, other features included to the design were two cooling fans which introduced convection; one fan pushed while the other pulled convective air, and reduced the amount of heat conducted to the mounting block. The CAD model for this TWE apparatus can be seen in Figure 14. One of the challenges that came out of the second apparatus were developing the controls for the added components, this was

possible with the association of another student who was heavily involved in the programming and wiring of the components onto a control box, shown in Figures 15 and 16.

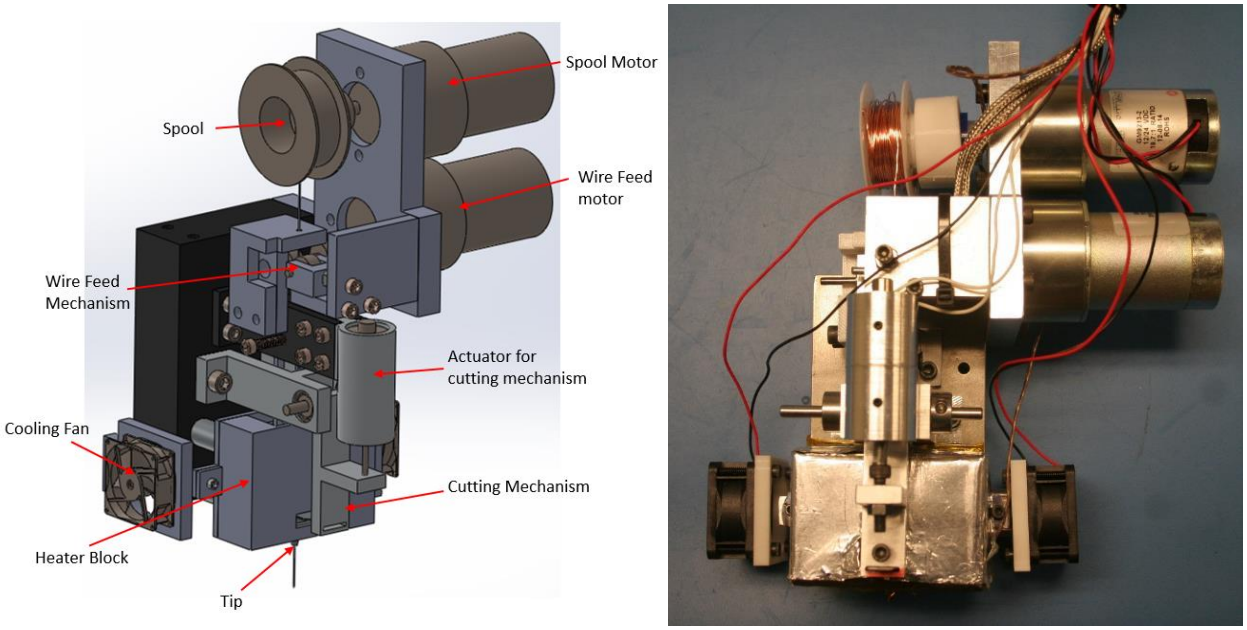

Figure 14 – Isometric view of second TWE CAD model (left). Actual view of second TWE tool (right).

Figure 15 – Thermal Wire Embedding Tool Control Box

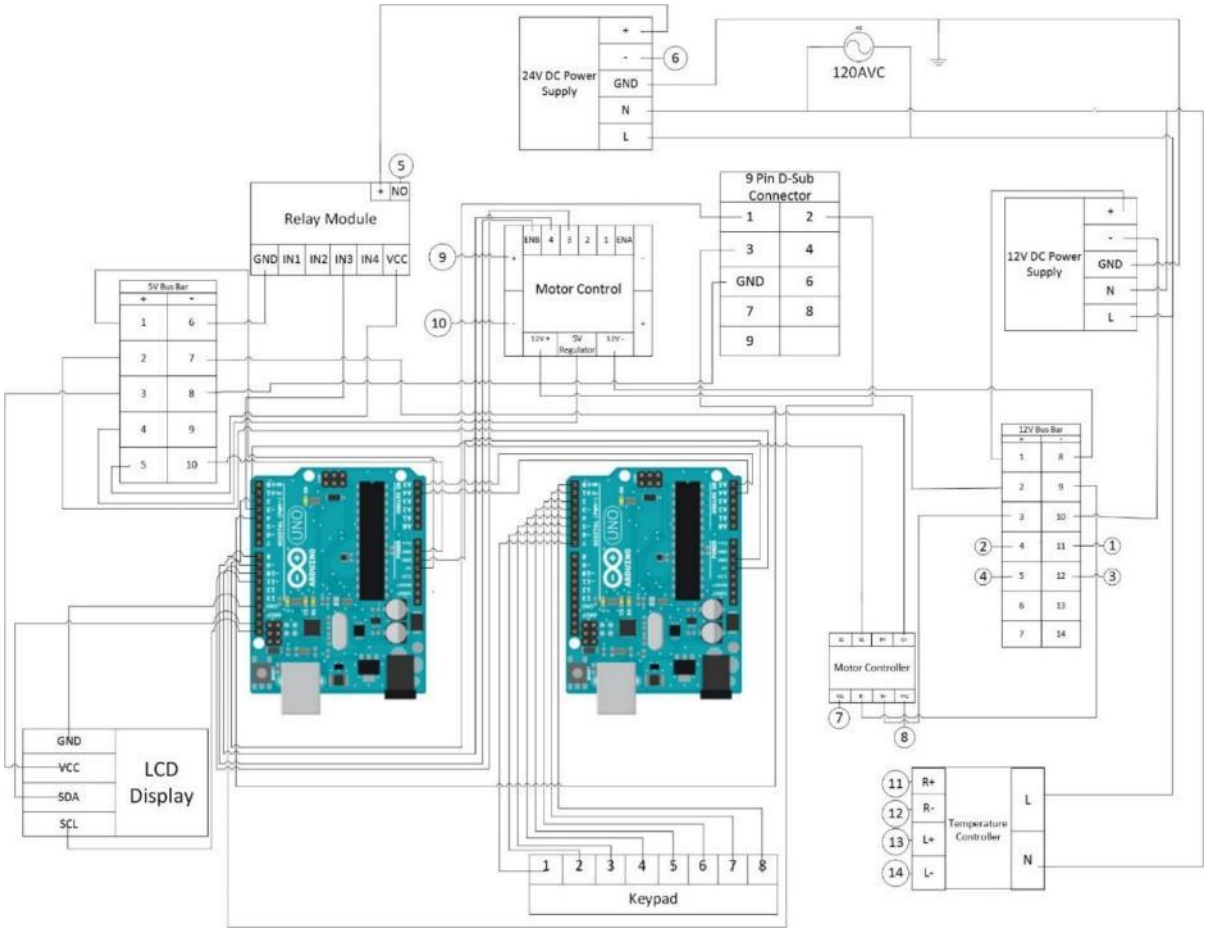

Figure 16 – Wire diagram of TWE Tool Control Box

In collaboration with Lockheed Martin Space Systems and Wolf Robotics, we were able to push the TWE apparatus through the required challenges to achieve a more fully automated process. The project involved a new system which uses industrial robots to fabricate a part using a material extrusion process as well as introduce other technologies that can be involved with the building process. The objective for this project was to install the TWE tool onto an industrial robot and embed 22 gauge wire on a PolyOne Carbon Fiber ABS (13% Carbon Fiber, ABS base polymer) composite provided by Lockheed Martin Space Systems. This project exposed the TWE tool to a virtually limitless space to embed wire in the working envelope. The challenges for this project were, limiting the weight of the TWE head to less than 20 lbs., developing parameters for the PolyOne Carbon Fiber ABS composite, experiment with the added features to the TWE tool, as well as developing a method that will embed wire onto the part without any human involvement.

For embedding wire, the second TWE tool involved a similar process than that of the prototype tool. Developing the approach to embed wire was required due to the addition of the motors and cutting mechanism. This process required to correlate the motors to feed and rotate the spool of wire in sync with the traverse speed of the motion control system. The motors did not include an encoder to generate any feedback or information of the motor's performance. Only if the driver motor introduces tension by driving the wire will the motor with the spool of wire rotate. Signals were generated to command the motors to rotate with the addition of the control box and microcontroller. The signals to energize and de-energize the components were toggled by directing the microcontroller to send the commands when desired. The microcontrollers used were two Arduino UNO which communicated via I^2C.

The modified method used to embed wire with the second TWE tool involved using the same method to measure offset dimensions as the former, as well as generating a G-code with further modifications to include commands for the two motors and the cutting actuator. For the second TWE tool, a staking method was developed that can be seen schematically in Figure 17. Once ready to embed, the TWE tool approached the plastic surface, without or with a desired amount of lead wire outside the tip's orifice, until the orifice is submerged a certain distance into the thermoplastic surface. While in the plastic surface, a dwell was implemented to melt or soften the plastic. The motors were then signaled to operate for a given time that would allow the wire to advance from the tip's orifice into the softened plastic so that the wire was submerged further. After the wire was driven further into the substrate, the TWE tool then moved away from the surface of the plastic at the same speed that the motor was driving wire until the TWE tool had moved a certain distance away from the surface. Once the head had moved a certain distance away from the surface, the motion away from the surface stopped, as well as the motors. Following was a supply of cool air from the convective cooling hose to help solidify the softened plastic and encapsulate the wire. This process created the initial stake of the wire which provided the strength required in the solidified plastic to mitigate the wire from detaching as the TWE tool advances from the starting point. The heated tip will then be brought back to the plastic surface, with the

feed motors engaged simultaneously as the TWE head moves. The tool immediately traverse as it comes into contact with the surface away from the initial pattern position and continue along its desired toolpath. If a corner is desired to be created with the wire pattern, a similar step as the initial stake of a trace is required. As the TWE tool approaches the point which will create the corner, the TWE must submerge itself as it does in the initial stake. Once submerged the TWE head must stop as well as the motors and dwell in order to soften the material and begin another staking point by feeding wire further into the substrate. After a dwell, the TWE tip ascends away from the surface as the motors continue to feed. After moving away from the surface the TWE head and motors are required to stop and initiate the blast of cool air in order for that point to solidify and continue the wire pattern. Once cooled the TWE orifice can come back into contact with the surface again to continue the embedding process. Each point that is designed in the wire pattern must perform the staking method in order to achieve the wire embedding goal. The final point, with stake and provided cooling, will conclude with actuating the cutting mechanism in order to terminate the trace.

Figure 17 - Wire embedded into substrate

The second TWE apparatus was able to successfully eliminate any human involvement during the wire embedding process. After utilizing the TWE tool for various trials, some deteriorating was noticed on the aluminum heated block, particularly where it clamps and encased the stainless steel tip. The tip deflected as it was embedding across a substrate and began to pry on the heated block. Considering the temperatures the TWE head operates in, the

aluminum block began to fail and the tip diverged from the concentricity that is required to keep the tool head perpendicular to the surface it is embedding on. These material and design issues were addressed in the final TWE tool that was developed.

4.2 THE FINAL THERMAL WIRE EMBEDDING APPARATUS DESIGN

The previous revision of the TWE tool design successfully eliminated any human involvement during the wire embedding process but it had some need for improvement when it came to maintenance, assembling/disassembling, and durability. The following design altered some of the previous design's features by changing the heated blocks aluminum body to a stainless steel body in order to improve on the durability of the tool. The cooling fans and the spool motor were removed in efforts to reduce the volume of the tool. The previous design had steel spacers sandwiched between the mounting block and the heated block, with the aid of the fans to reduce the heat conducted to the mounting block. Since the fans were removed, the steel spacers were replaced by grade L5 ceramic spacers to mitigate the heat transfer to the mounting block from the heated block. The spool motor was not seen to have much of an influence on the wire embedding process. The only need that was noticed for the spool motor was when the wire was retracted from the tool back on to the spool. This step was not essential to the wire embedding process. Since the spool motor was removed a one-way bearing replaced how the spool of wire was installed and fed. The one-way bearing minimizes the friction of the spool of wire when it is pulled to feed and subsequently rotate the spool. The CAD model of the final TWE tool's design can be seen in Figure 18.

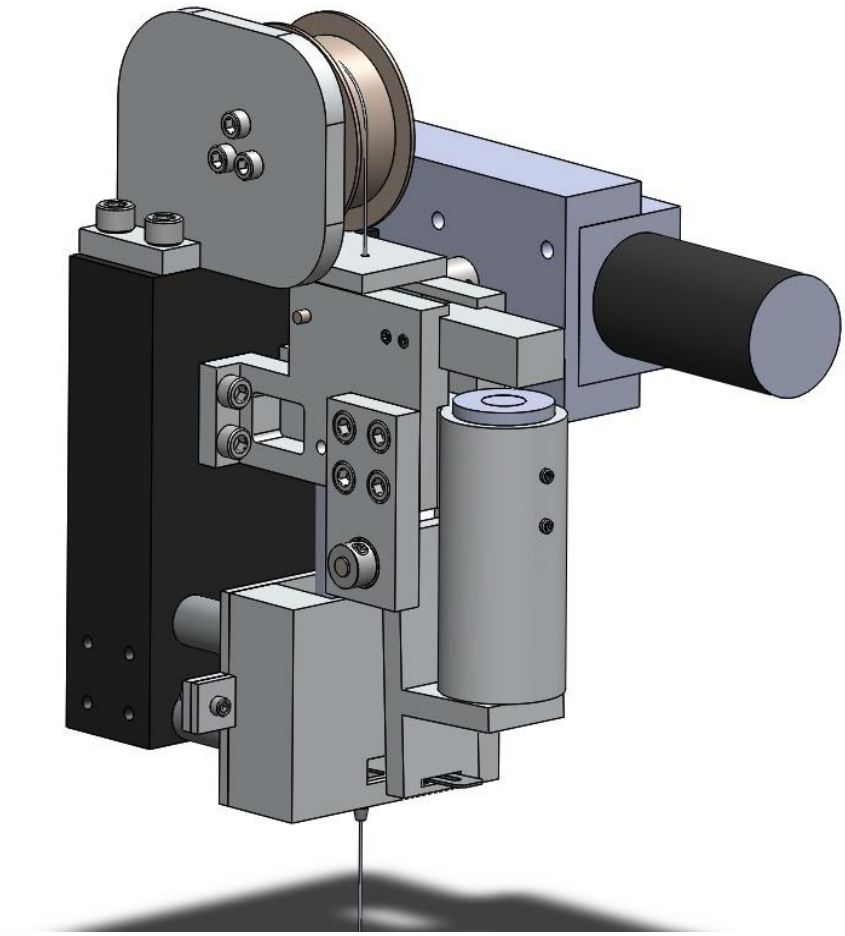

Figure 18 – CAD model of the final TWE tool design

The new design also used a right angled 12V DC motor to condense the volume of the tool. Other feature changes simplified the assembling/disassembling of the tool as well as helped in the maintenance of the tool. Some of the changes in the design were re-designing the pinch roller system to become more modular and simpler to replace. There was also a redesign of how the cutting mechanism's T-shaped pivot arm is mounted to allow replacing the cartridge heaters without disassembling the entire driving and cutting mechanisms. This tool was installed on an LC 3024 CNC router (Techno, Inc., New Hyde Park, NY, USA) and used to measure the accuracy of the wire placement. The position of the TWE tool was orientated in a way where the normal of the front face of the TWE tool is parallel to the –X direction of the gantry. The method used to embed wire remained the same as the previous method used with the second TWE design.

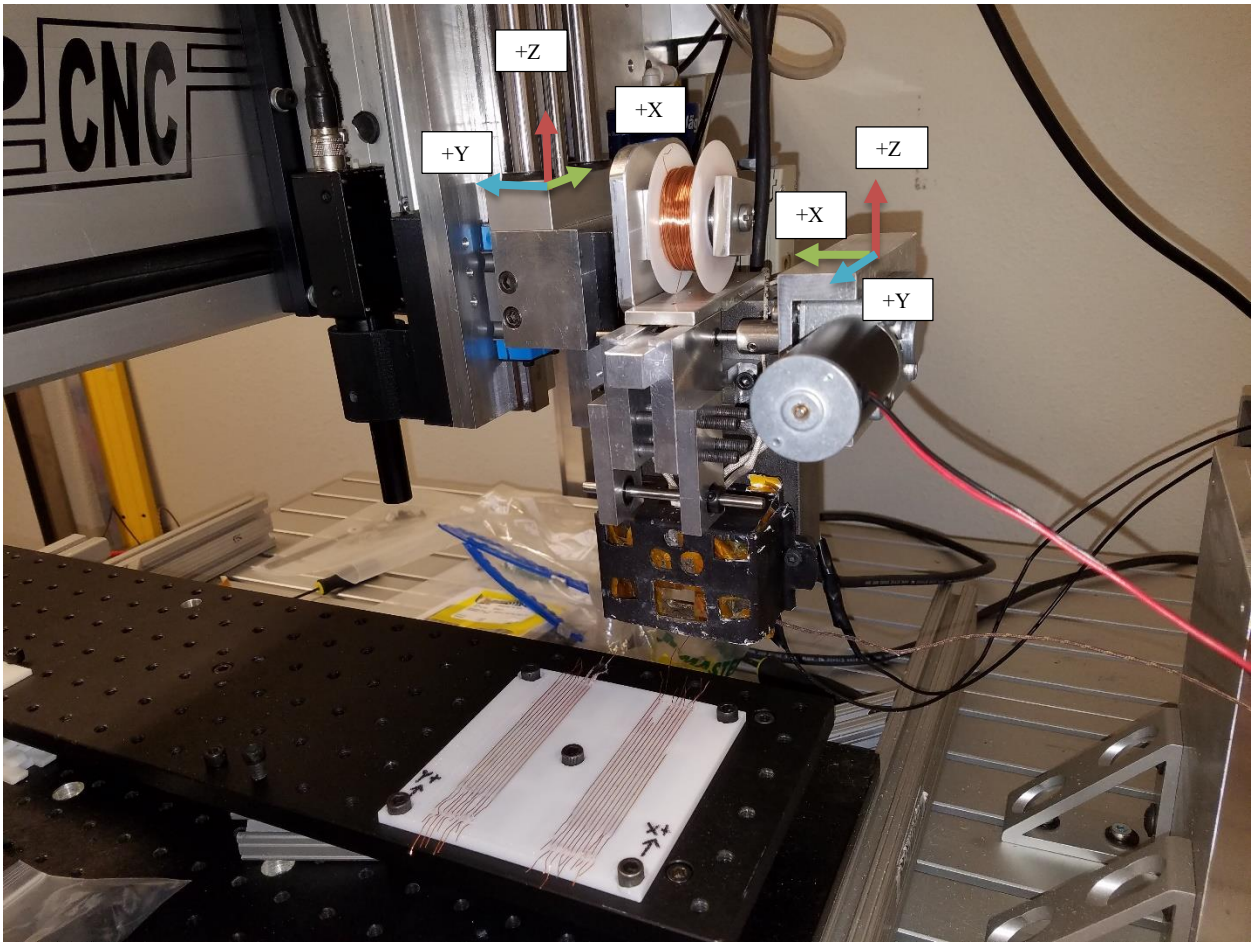

Figure 19 – Final TWE apparatus mounted in -90˚ orientation on Techno CNC router

Chapter 5: Applications for the Thermal Wire Embedding Apparatus for FDM-Printed Parts

5.1 UAV PROJECT

The TWE tool was used to deposit 32 gauge wire on a nylon FDM printed substrate. The wire pattern consisted of 3 straight wires that were embedded with wire of lengths over 100 mm long and 6 wire traces that were each designed with a 90 degree turn. The challenges during this process were associated with the designed spacing of the wires, experimenting with wire embedding on nylon FDM printed substrates, as well as overcoming some of the thermal-induced warping the printing sheets and parts were displaying. Warping on these parts were visually obvious as the nylon parts were taken out of the FDM printer. It was apparent that the warping occurred on these parts because of their slender build size, the thickness at the point of embedding wire was 1.016 mm (0.040”), with the warping shown in the image to the left in Figure 20. The warping hurdle was subdued by increasing the thickness of the part to 8.89 mm (0.350”) at the point of embedding wire and by gradually introducing the FDM-printed parts to room temperature levels, which is the temperature the thermal embedding head was operating in. The positioning of the embedding lines were designed to be 2.591 mm spaced apart from each other. The challenge that the spacing of the lines presented was that during the 90 degree turns, the G-code had to strategically include offsets and pauses during the translation in the adjacent direction. Determining the temperature for embedding copper wire on nylon substrates was done in the same trial and error fashion as on the PC substrates. Noticeable surface damage was also seen by the heat affected zones when experimenting with the tool height offset. Traverse speeds in the G-code were kept at a minimum of 1 mm/s as well. The embedded wires were used as interconnections for electronic components designed for a 3D FDM printed UAV. The UAV fuselage wiring was incorporated using the prototype TWE tool. Therefore, all the manual tasks associated with that tool were performed here (e.g., manual gripping and shearing wire). The G-code was programed to embed all wire tracks in one process so it was important to add dwells (pauses), of at least 5 seconds, between the different wire tracks to ensure that the user can prepare for the initial process

of a wire embedding track as well as enough time to shear the wire of each wire trace. Once the wire embedding process concluded the Nylon specimens required a post-process which consisted of trimming the excess wire leads in order to allow the FDM printer to resume the 3D printing build. The following images show the results of the work and process described. This work was done in association with another student from The University of Texas at El Paso (UTEP) in the W. M. Keck Center for 3D Innovations and this link is a reference to more details of the work as well as the final product; also shown on the image on the right in Figure 21 (https://www.youtube.com/watch?v=jk5z1Tbqdno).

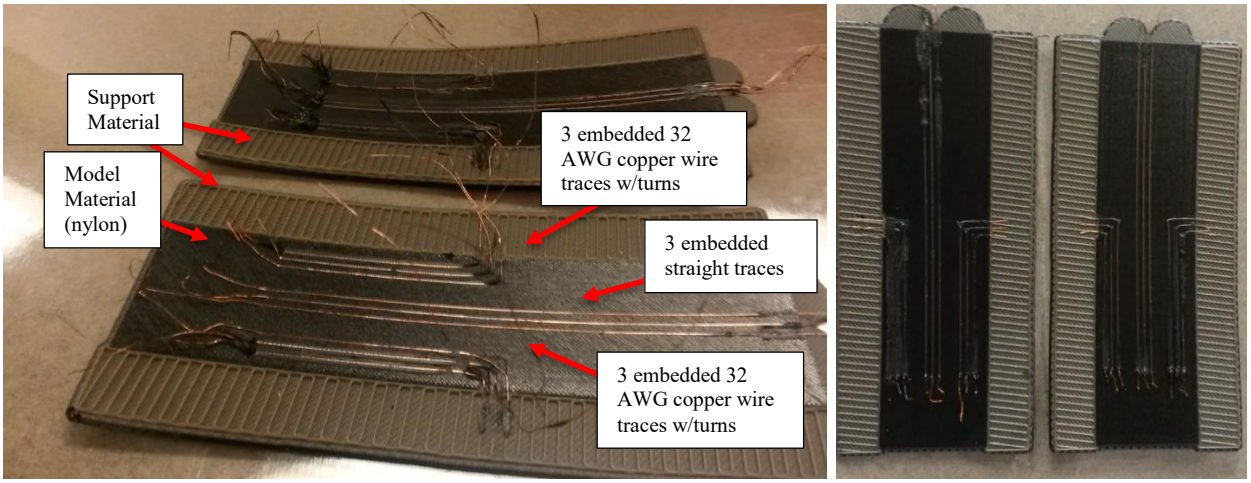

Figure 20 – Two partially built FDM printed (nylon) UAV fuselage w/ 32 AWG copper wire. Note the warping, induced from the wire embedding process (left) and successful results (right).

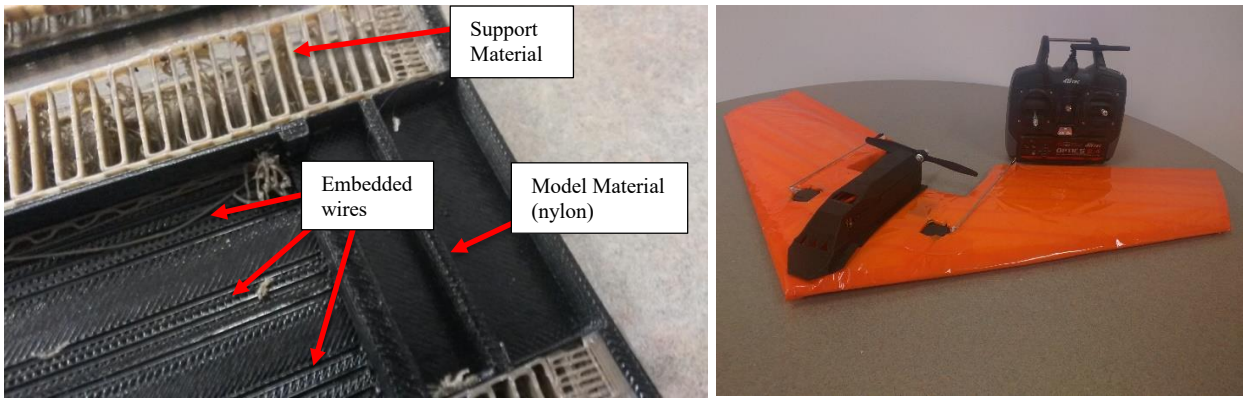

Figure 21 – 32 AWG copper wire printed over for a FDM-printed UAV fuselage (left). Actual view of a FDM-printed UAV (left).

5.2 EMBEDDING NICKEL-CHROMIUM WIRE

Successfully being able to embed copper wire with great repeatability led to an attempt of embedding 28 gauge Nickel-Chromium (Ni-Cr) wire. Ni-Cr 80/20, a non-magnetic alloy of nickel and chromium, was proposed due to its excellent resistance to high temperature oxidation and corrosion, good wear resistance, stiffness, and good strength ("NiChrome - Nickel Chromium Alloys." http://nickel-alloys.net/nickel_chrome_alloys.html). Nickel Chromium is widely used as an electric heating element and even in dentistry. (Louise McGinley, 2011). Due to the materials resistance to oxidation, when conducting electricity, it is the most common resistance wire used for heating purposes (i.e. electric room heaters, toasters, stove top burners, and such things alike). The resistance wire's high hardness and good corrosion resistance contribute to the materials good wear resistance (Woolf, 2002).

Figure 22 – Initial Ni-Cr wire embedding results

In order to embed Ni-Cr wire into PC substrates, test and parameter developments were implemented (initial results shown in Figure 22, successful results shown in Figure 23). The Ni-Cr wiring was incorporated using the prototype TWE tool. Therefore, all the manual tasks associated with that tool were performed here (e.g., manual gripping and shearing wire). Similar to the parameter development of copper wire, Ni-Cr wire required its own temperature manipulation. By maintaining the 1 mm/s feed rate in the embedding process, the temperature values were required to increase due to the lack of thermal conductivity the Ni-Cr (12W/m*K) wire has in comparison to the copper (401 W/m*K) wire (Çengel, 2011).

Embedding a stronger metal wire (Ni-Cr) on a FDM printed thermoplastic specimen required some preliminary runs before being able to successfully embed some of the generic patterns produced previously with the copper wire. After some experimenting on PC substrates, the parameters were developed and repeated embedding results were achieved. The method developed proved that the TWE tool can embed a stronger wire, compared to copper, and repeated embedding results were achieved which enabled testing the mechanical aspects of metal wire on a FDM printed thermoplastic specimen.

Mechanical testing consisted of PC FDM-printed specimens that were exposed to tensile testing. The test were carried out using the ASTM D638 Type 1 standards (Ref ASTM D638 Type 1). A sample group of 14 polycarbonate (PC) specimens were printed using a Fortus 400mc (Stratasys, Inc., Eden Prairie, MN). Due to the interfacial bonding between the layers, the layers can separate from one another much easier when tensile pulling a specimen in the Z direction. It is important to note that these tensile specimens were printed in the Z direction, as compared to the building in the XY plane leaving the Z direction of the build to be the shortest, making it the weakest orientation these specimens can be printed in using the FDM technology. Half of the specimens, 7, in this batch were used as a control group (i.e., these specimens were not introduced to the TWE process). The other half, 7, of the specimens were each introduced to the TWE process (see Figure 23). The specimens that underwent the TWE process were embedded with a total of

10 traces of Nickel-Chromium wire each and with the same wire pattern. The two wider faces of the specimens were utilized to embed 5 tracks of Nickel-Chromium wire on each face. Only 5 of the specimens that were meant to be embedded with Nickel-Chromium were considered successfully embedded. Due to the human involvement required for this process of embedding wire utilizing the prototype TWE tool, this created some deviation in 2 of the specimens that were considered not fully embedded with the Nickel-Chromium wire pattern. Even though not all of the specimens were considered fully embedded with 28 gauge Nickel-Chromium wire, 5 of the specimens were successfully fully embedded with 28 gauge Nickel-Chromium wire. The control set and wire embedded specimens were also conditioned for 40 hours at 23 ºC and 50% relative humidity, according to the ASTM standard D618 (Ref ASTM D618). Tensile tests were performed to measure how the mechanical properties can be altered when using the TWE technology to introduce a wire pattern on an FDM-printed part.

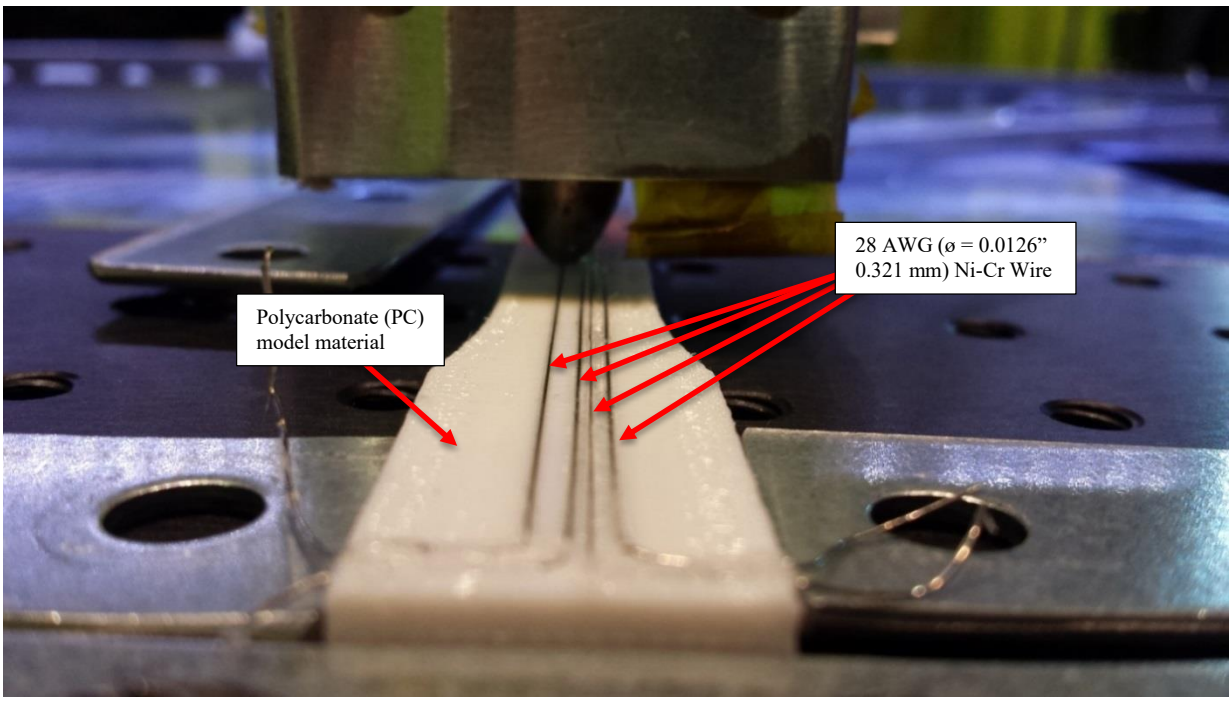

Figure 23 – Embedding Ni-Cr wire on tensile specimen

5.3 LIVE DEMONSTRATIONS PERFORMED WITH THE SECOND TWE TOOL

Using the Multi-Robot Additive Cluster System developed by Lockheed Martin Space Systems and Wolf Robotics, UTEP participated in a project that included performing a live demonstration with the TWE tool. One live demonstration was performed at FABTECH 2015 in Chicago, IL and another live performance was done at the Defense Manufacturing Conference (DMC) 2015 in Phoenix, AZ. Both demonstrations were performed successfully and allowed to showcase the multi-functionality that can be added to a FDM-built structure. The following figures (Figure 24 and 25) show the results of those events. Figure 25 shows a FDM-built motion detector utilizing the embedded wires.

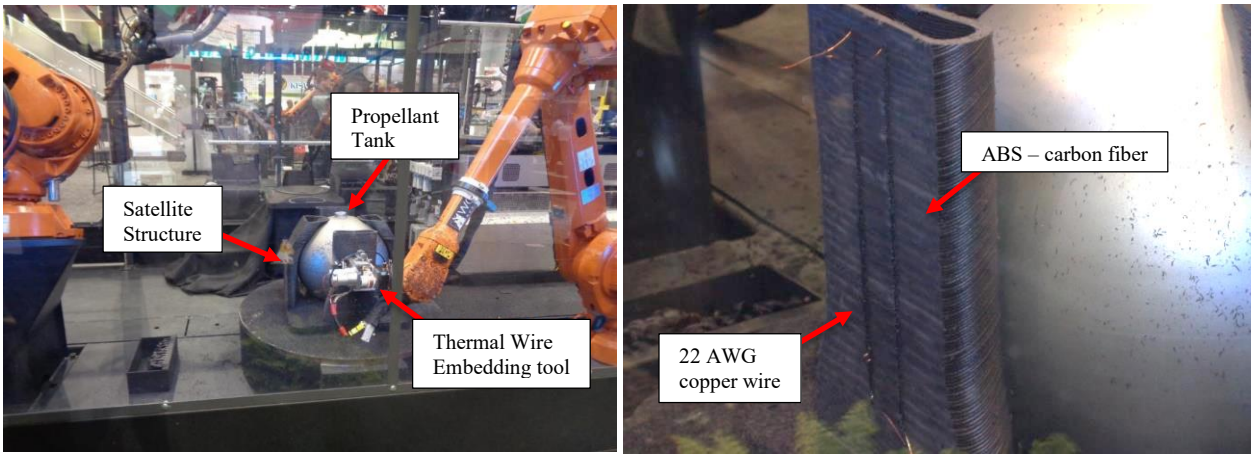

Figure 24 – The TWE tool installed on the Multi-Robotic Additive Cluster System at FABTECH 2015. 22 AWG copper wires embedded on a satellite structure.

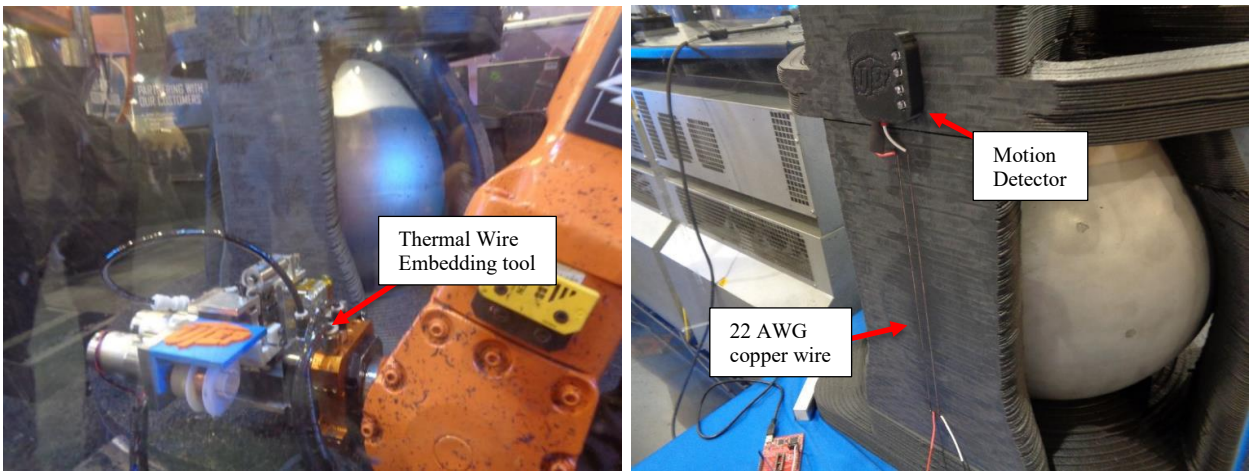

Figure 25 – The TWE tool embedding 22 gauge copper wire on a satellite structure at DMC 2015. A FDM built motion detector installed on a satellite structure

Chapter 6: Results of embedding wire using the Thermal Wire Embedding tool

6.1 Results for Ni-Cr wire embedded specimens on PC material

Tensile tests were performed using an Instron 5866 (Instron, Norwood, MA) tensile testing machine. The results revealed that the Ni-Cr wire embedded specimen's Young's Modulus, ultimate tensile stress, and elongation all increased when compared to the control set. Due to how the tensile specimens were built, ZXY orientation, the curves only show elastic deformation (straight line). There is no presence of plastic deformation (nonlinear deformation). Results obtained from the tensile tests are presented in Figures 26 and 27. The tensile test results for the control group are comparable to previous tensile test performed to the ZXY built tensile specimens resulting in Young's Modulus averaging 1801 MPa, UTS ranging from 16.4 MPa to 21.5 MPa, and tensile strain of 1.6% (Hossain *et al.*, 2014).

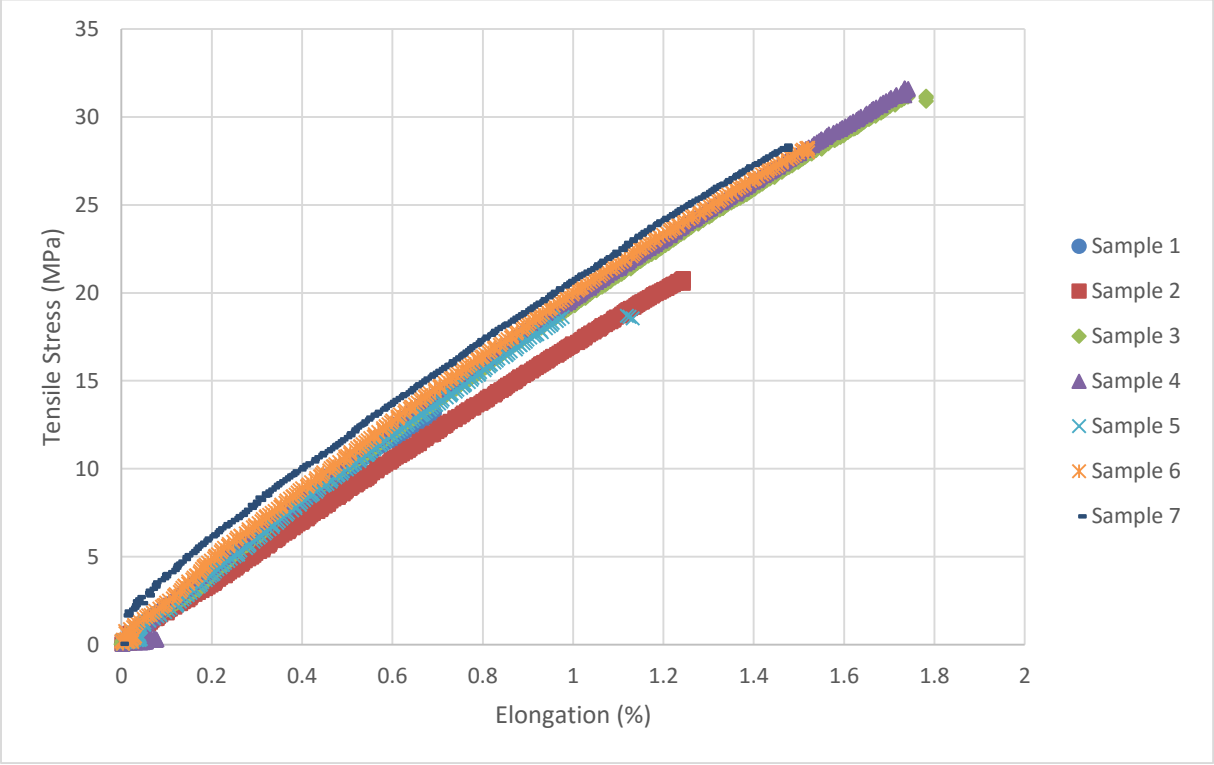

Figure 26 – Stress-strain curve for control group

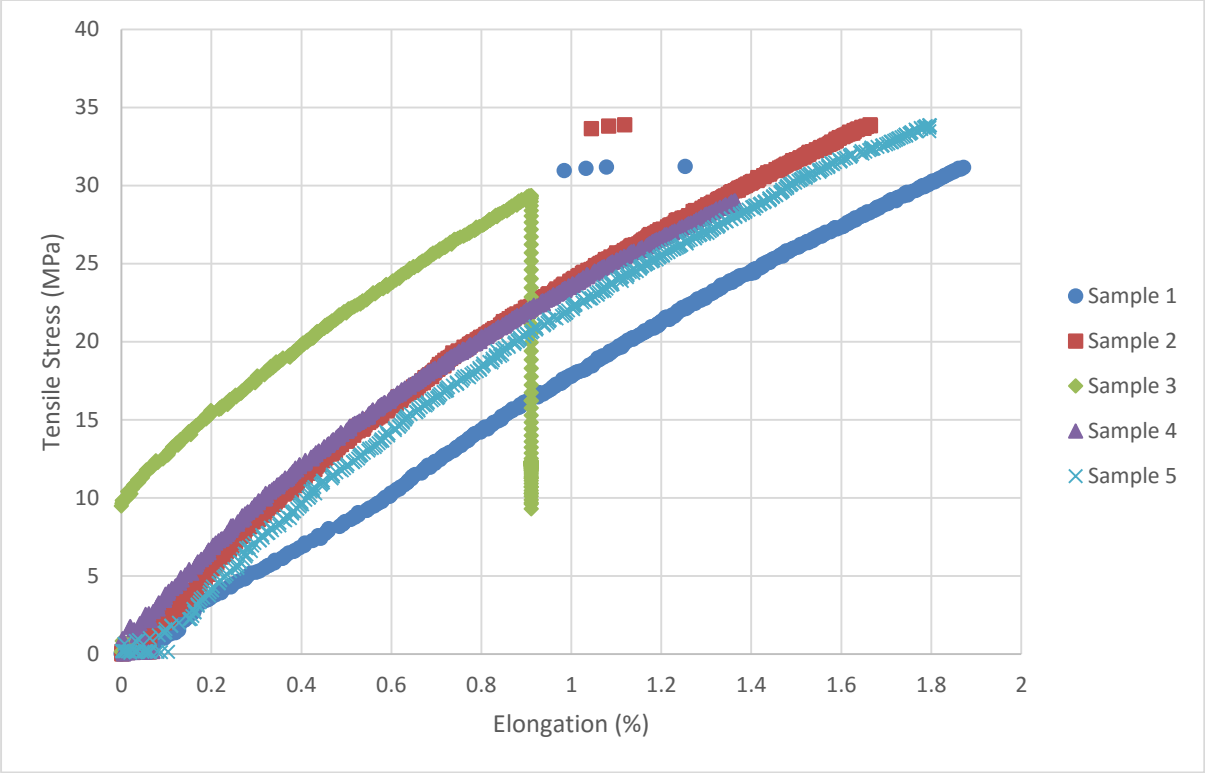

Figure 27 – Stress-strain curve for Ni-Cr wire embedding group

Examining the data (Figure 28) showed that the Ni-Cr wire embedded specimen results had a large standard deviation on the Young's modulus. The large variable that may have played a role to the deviation may have been due to the human involvement required to embed wire to these specimens. The deviation seen in the UTS for the specimens embedded with the Ni-Cr wires decreased when compared to the control set specimens. The decrease in the deviation might be caused by the change in surface roughness caused by the TWE process. The TWE tool might be homogenizing the path in which it is traveling as it is removing a section of the visible seam lines. The average Young's modulus, UTS, and elongation of the seven PC specimens of the control set yield 2107 MPa, 24.61 MPa, and 1.37% respectively. The Ni-Cr wire embedded specimen's resulted with 3064MPa, 31.47 MPa, and 1.52% for the Young's modulus, UTS, and elongation respectively. Overall a 45% increase in Young's modulus, an increase of 28% in UTS, and an 11% increase in elongation by embedding Ni-Cr wire to a PC substrate. These results can possibly be increased by embedding a different pattern as well as by using the fully automated TWE tool to remove any human involvement.

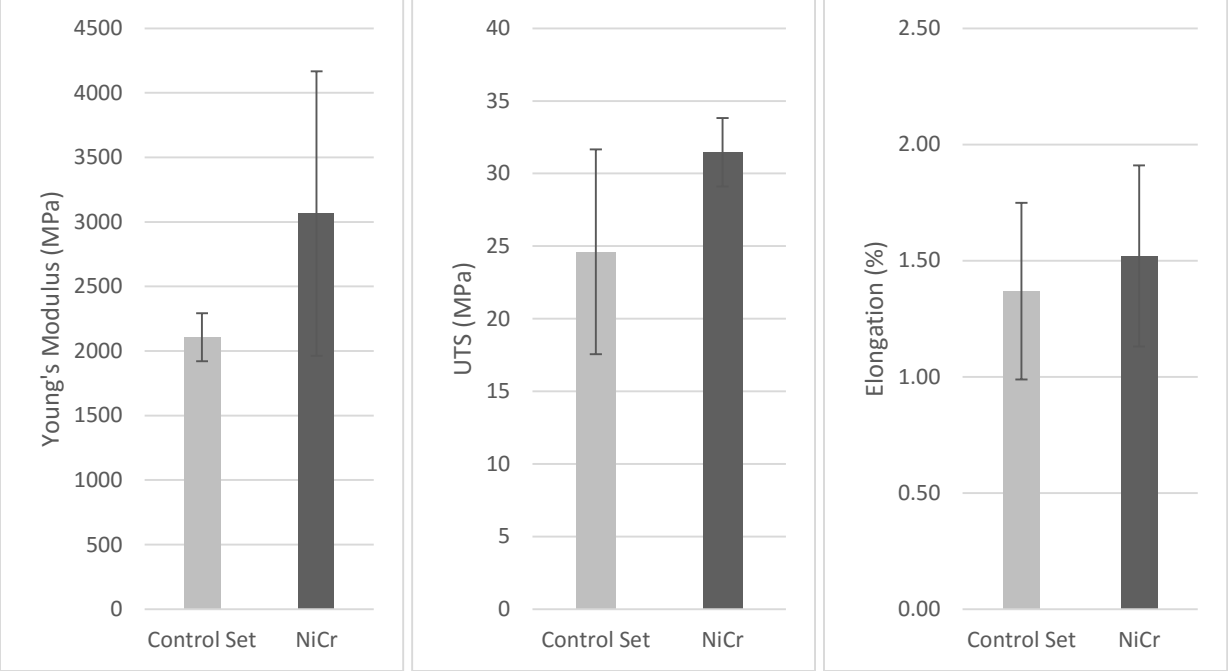

Figure 28 – Average results of the control set and Ni-Cr embedding specimens. Averages were based of least five measurements and error bars represent +/- one standard deviation.

6.2 RESULTS OF CONTINUITY TEST PERFORMED WITH THE FINAL TWE TOOL

A continuity test was performed on 28 AWG gauge copper wires embedded onto PC substrates. The purpose of this test was to measure how close the wires can be embedded next to each other before continuity is seen using a digital multi-meter. The 28 gauge copper wires were embedded as close as 0.5 mm apart, specified in the CNC interface system. Figures 29 shows the results of the embedded wire on the left and a magnified close up of the wires on the right. Table 6.1 shows the results of the continuity test.

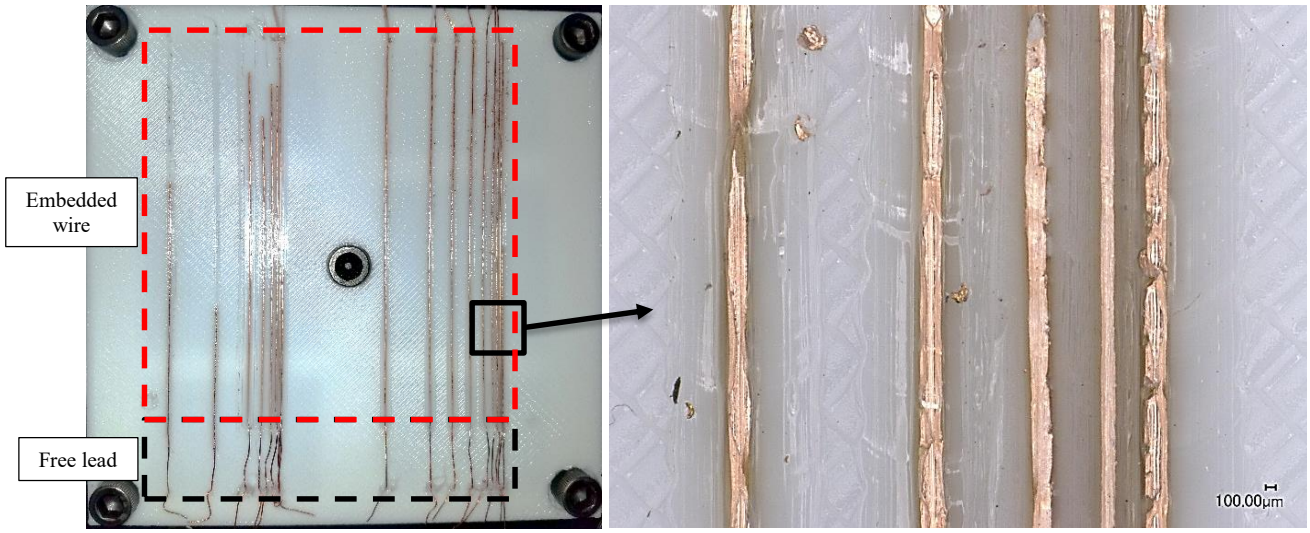

Figure 29 – 28 AWG embedded copper wire for continuity test. Image on right shows 50x magnification of wires spaced 2mm, 1mm, 0.75mm, and 0.5mm respectively apart.

Table 6.1 Conductive Coupling Test of 28 AWG (Ø = 0.0126" 0.321 mm) copper wire

Spacing between wires	Conductive coupling
10 mm	NO
5 mm	NO
4 mm	NO
3 mm	NO
2 mm	NO
1 mm	NO
0.75 mm	NO
0.5 mm	NO

The results show that conductive coupling is not seen for wires that are spaced 10 mm, 5 mm, 4 mm, 3 mm, 2 mm, 1 mm, 0.75 mm and 0.5 mm apart from each other. Embedding the wires

closer than 0.5 mm apart was not possible due to the wire shearing as the lines are spaced closer. This could be due to the copper wire previously embedded acting as a heat sink and not allowing the new wire to successfully be embedded.

6.3 Results of Positional Accuracy measurements for the Thermal Wire Embedding Tool

This test allowed us to measure the accuracy of the placement of the wire. Figure 19 shows the set-up of the TWE tool on the CNC router. It should be mentioned that the orientation of the tool again is rotated -90˚ in reference to the CNC routers orientation. Figure 30 shows the work piece with 100 mm length 28 AWG copper wires embedded into it and were designed to be spaced 2 mm apart. Additionally, Figure 30 highlights the initial, middle, and final portions of the embedded lines with colored frames corresponding to their graphical representations. The wires on the left half of the work piece were embedded from the bottom to the top of the part (+Y of the CNC router). The work piece was then rotated +90˚ in order to measure the positional accuracy of the +X direction of the CNC router and were embedded from left to right. A cut with a 0.020” end mill was created in order to have a reference line when measuring the positional accuracy with the Smartscope Flash 250 (Optical Gaging Products Inc. Rochester, NY). The first 20 mm were measured as the initial portion of the embedded wire, the following 60 mm of the wires were measured as the middle portion of the wire, and the final 20 mm of the wires were measured as the end portion of the wires. The results are shown in Figures 31.

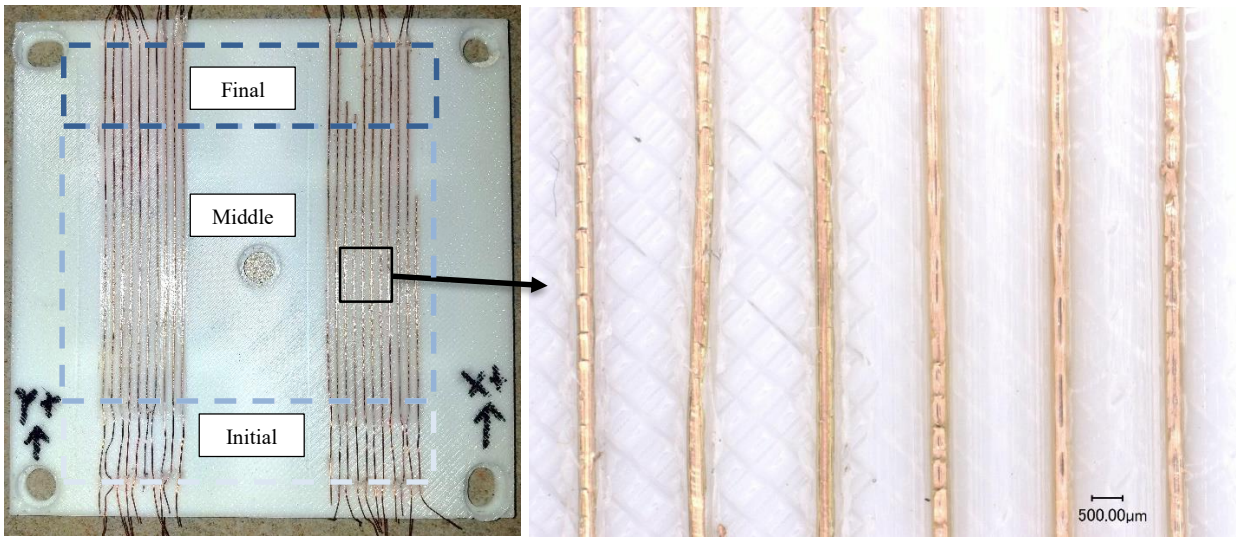

Figure 30 – 2 mm spaced 28 gauge copper wires for position accuracy measurements. 30X magnification of wires

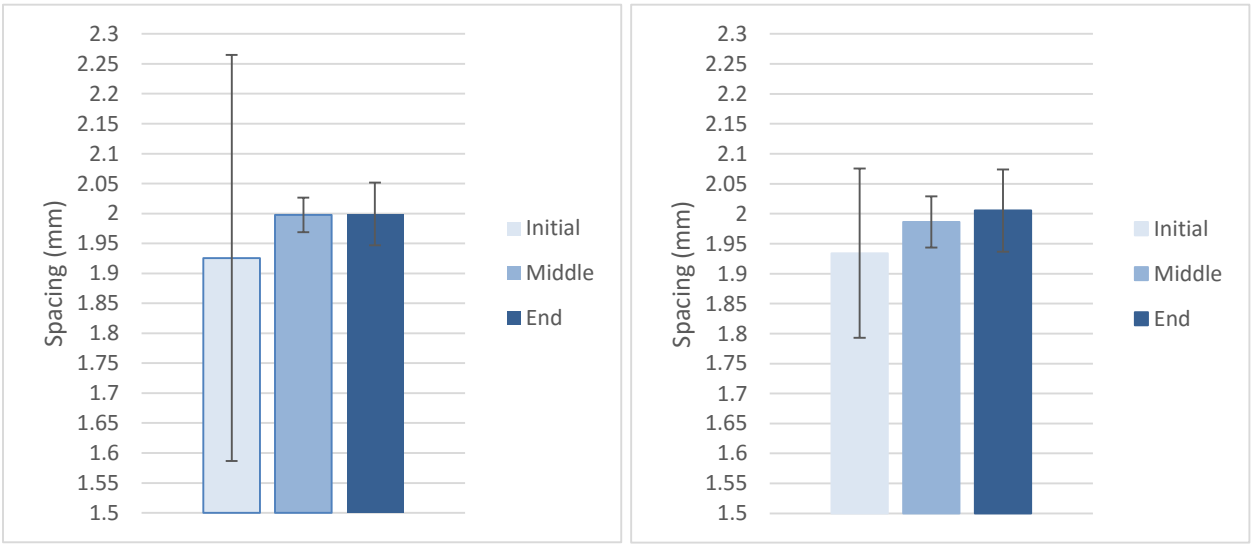

Figure 31 – Results of average copper wire positional accuracy. Y+ results (Left). X+ results (Right). Averages were based of least five measurements and error bars represent +/- one standard deviation.

The results show that the initial portion of the wires varied in both the X and Y direction of the embedded wires with a large deviation when compared to the middle and end portions. This deviation is largely caused by the initial staking point and ascend method of the wire embedding process. The middle and end points show that the wires are more accurately spaced from each other with much smaller deviations. Table 6.2 displays the results of the positional accuracy test.

Table 6.2 Average results of Positional Accuracy

	Average +X Values	σ (+/-)	Average +Y Values	σ (+/-)
Initial	1.934	0.141	1.926	0.339
Middle	1.986	0.042	1.998	0.029
End	2.005	0.068	1.999	0.052

6.4 RESULTS OF STRAIGHTNESS TEST OF DIFFERENT GAUGE WIRES

This test was done to measure the straightness of the wires being embedded in a straight line. The tip of the TWE tool has a fixed exit diameter of 1.016 mm (0.040”). If the gauge of the wire is changed the area between the edge of the orifice and the outer diameter of the wires also varies. The clearance allows the wire to move or shift within the inner diameter of the exit orifice. This is important to know from a design standpoint due to the constraints that can come from the results of these measurements. Measurements were taken for four different gauge wires, Figure 32 and 33 show the results of the embedded wires.

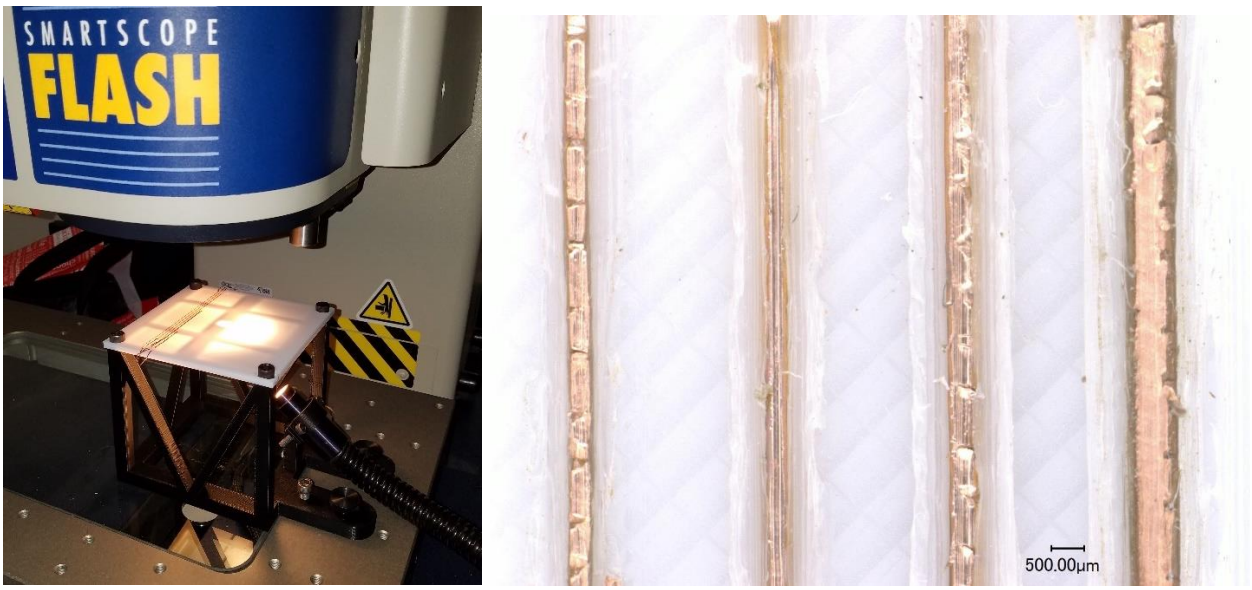

Figure 32 – Different gauge wires being measured with the Smartscope Flash 250 (left). 50X magnification of 30, 28, 26, and 24 gauge embedded wires on PC (right)

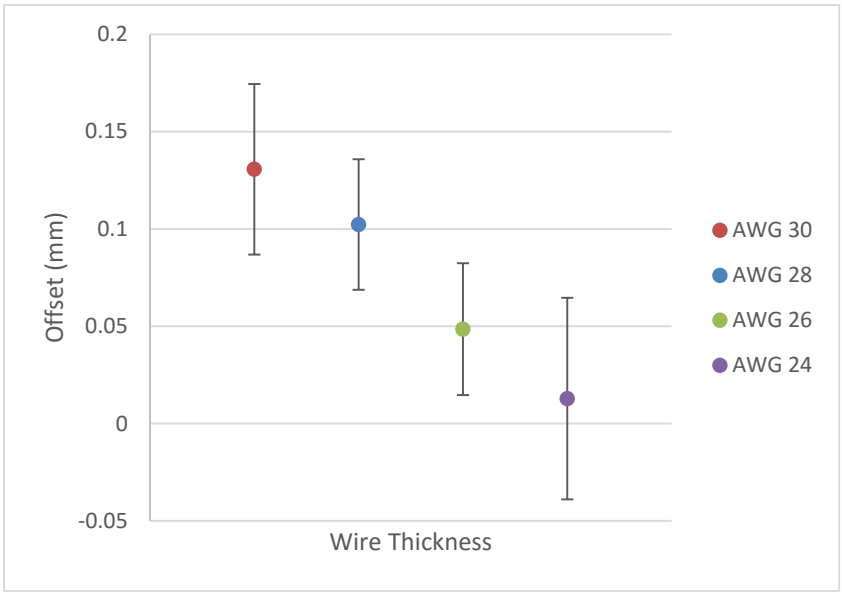

Figure 33 – Results of average offset measurements for different gauge wires. Averages were based on five measurements and error bars represent +/- one standard deviation.

The results do show that as the diameter of the wire increases the offset from it being a straight line decreases. The thinner wires have more area to move around the orifice as it is exiting the tip. This can be remedied by designing smaller orifice tips for thinner wires.

Chapter 7: Conclusions and Future Work

7.1 CONCLUSION

The thermal wire embedding tool was designed and developed to embed metal wires onto FDM-printed parts. The design of the TWE tool was iterated and manufactured through a few revisions. The designs were evaluated through its use and results of the experiments and determined the functionality of the state of the designs. The modifications to the designs improved the functionality of each design iterations.

The TWE was able to be modified to become fully automated and remove any human intervention in the wire embedding process. The use of a DC motor and pinch wheel driving system allowed to drive the wire as required throughout the wire embedding process. The design of the pinch wheel drive system allows the rollers to be modular and easily interchangeable to drive various gauge wires. The utilization of an electric push solenoid with a cutting mechanism which includes off-the-shelve commercial blades allows to shear the wire and terminate a trace as needed. The method to embed wire using the TWE tool was experimentally developed and was able to be repeated with different gauge wires as well different material type of wires. When embedding 28 AWG copper wire and utilizing the final version of the TWE tool, the wires were able to be placed as accurate as +/- 29 μm of its desired position using the Techno CNC router. The use the copper wires on FDM-printed parts demonstrated that they can be used as conductive traces for electronic applications. Inherently as we embed wire with the TWE tool we increase the mechanical properties of the FDM-built structure. Embedding Ni-Cr wires on PC parts can increase the Young's Modulus and UTS by 45% and 28%, respectively. It is also seen that it is required to change the tip with an appropriate orifice to correlate with the wire gauge in order to maintain a straighter path for the wire to be embedded in.

7.2 FUTURE WORK

A large amount of success was achieved during the timeframe of this work but future work with the thermal wire embedding process is still required. Creating a software to generate

the toolpaths for the thermal wire embedding process from a CAD model to start would be an important tool in order to achieve toolpaths of various design patterns of wire in a shorter amount of time. Manufacturing different tips for their appropriate wire gauges should be considered if accuracy is greatly required. Further development on the method for embedding different gauge wires would be suggested in order to accelerate the process when transitioning to different gauge wires and also when embedding on different material type parts. Incorporating this tool onto other technologies has been shown to be fully capable with the Multi-Robot Additive Cluster System but it has yet to be incorporated to run a fully automated process with the Multi^{3D} system.

References

"1_Mil_Kapton_Tapes_Datasheet_ (KP)."

"3d Printed Electronics Applications." Neotech-AMT. http://www.neotech-amt.com/3d-printed-electronics-applications/.

Aguilera, Efrain et al. "3D Printing of Electro Mechanical Systems." *Proceedings of the Solid Freeform Fabrication Symposium*. 2013. 950–961. *Google Scholar*.

Ambriz, Steven Daniel. "Design and development of the portable build platform and heated travel envelope for the Multi3D manufacturing system" (January 1, 2015). ETD Collection for University of Texas, El Paso. Paper AAI10000784. http://digitalcommons.utep.edu/dissertations/AAI10000784

Anil, Ch., and R. Padma Sree. "Tuning of PID Controllers for Integrating Systems Using Direct Synthesis Method." *ISA Transactions* 57 (2015): 211–219.

ASTM B267-07(2013) Standard Specification for Wire for Use In Wire-Wound Resistors, ASTM International, West Conshohocken, PA, 2013, http://dx.doi.org/10.1520/B0267-07R13.

ASTM B3-13 Standard Specification for Soft or Annealed Copper Wire, ASTM International, West Conshohocken, PA, 2013, http://dx.doi.org/10.1520/B0003

ASTM B344-14 Standard Specification for Drawn or Rolled Nickel-Chromium and Nickel-Chromium-Iron Alloys for Electrical Heating Elements, ASTM International, West Conshohocken, PA, 2014, http://dx.doi.org/10.1520/B0344-14

ASTM D638-14 Standard Test Method for Tensile Properties of Plastics, ASTM International, West Conshohocken, PA, 2014, http://dx.doi.org/10.1520/D0638-14

Bailey, Sean A. et al. “Biomimetic Robotic Mechanisms via Shape Deposition Manufacturing.” *ROBOTICS RESEARCH-INTERNATIONAL SYMPOSIUM-*. Vol. 9, 2000. 403–410. *Google Scholar*.

Bayless, Jacob, Mo Chen, and Bing Dai. “Wire Embedding 3d Printer.” *Engineering Physics Department, University of British Columbia* (2010): *Google Scholar*.

Calvert, Paul. “Inkjet Printing for Materials and Devices.” *Chemistry of Materials* 13.10 (2001): 3299–3305. *ACS Publications*. Web.

“Cartridge Heater.” *Metal Finishing* 105.6 (2007): 65. *ScienceDirect*.

Çengel, Yunus A., Afshin J. Ghajar, and Mehmet Kanoglu. *Heat and Mass Transfer: Fundamentals and Applications*. New York: McGraw Hill Higher Education, 2011.

Chen, Danfang et al. “Direct Digital Manufacturing: Definition, Evolution, and Sustainability Implications.” *Journal of Cleaner Production* 107 (2015): 615–625.

Coronel, Jose Luis. "Multi3D system: Advanced manufacturing through the implementation of material handling robotics" (January 1, 2015). ETD Collection for University of Texas, El Paso. Paper AAI10000794. http://digitalcommons.utep.edu/dissertations/AAI10000794

Deffenbaugh, Paul Issac. "3D printed electromagnetic transmission and electronic structures fabricated on a single platform using advanced process integration techniques" (January 1, 2014). *ETD Collection for University of Texas, El Paso.* Paper AAI3636252. http://digitalcommons.utep.edu/dissertations/AAI3636252

DeNava, Erick et al. “Three-Dimensional off-Axis Component Placement and Routing for Electronics Integration Using Solid Freeform Fabrication.” *Solid Freeform Fabrication Symposium, The University of Texas at Austin, Austin TX, Aug,* 2008. 4–6. *Google Scholar*.

Dxf2gcode Software | SourceForge.net.

Espalin, David et al. “3D Printing Multifunctionality: Structures with Electronics.” *The International Journal of Advanced Manufacturing Technology* 72.5-8 (2014): 963–978.

Espalin, David. "Development of a multi-material, multi-technology FDM system for process improvement experimentation" (January 1, 2012). *ETD Collection for University of Texas, El Paso.* Paper AAI1533221. http://digitalcommons.utep.edu/dissertations/AAI1533221

“Functionalize F-Electric - Highly Conductive Filament | Functionalize.” http://functionalize.com/.

Gibson, Ian, David Rosen, and Brent Stucker. *Additive Manufacturing Technologies*. New York, NY: Springer New York, 2015.

Guo, Nannan, and Ming C. Leu. “Additive Manufacturing: Technology, Applications and Research Needs.” *Frontiers of Mechanical Engineering* 8.3 (2013): 215–243.

Gutierrez, Cassie et al. “CubeSat Fabrication through Additive Manufacturing and Micro-Dispensing.” *Proceedings from the International Microelectronics Assembly and Packaging Society Symposium*. (2011). *Google Scholar*.

Hossain, Mohammad Shojib. *Fused Deposition Modeling (FDM) Fabricated Part Behavior under Tensile Stress, Thermal Cycling, and Fluid Pressure*. (2014). *Google Scholar*.

Mohammad Shojib Hossain, "Fused deposition modeling (FDM) fabricated part behavior under tensile stress, thermal cycling, and fluid pressure" (January 1, 2014). ETD Collection for University of Texas, El Paso. Paper AAI1564676. http://digitalcommons.utep.edu/dissertations/AAI1564676

Hossain, Mohammad Shojib, David Espalin, et al. “Improved Mechanical Properties of Fused Deposition Modeling-Manufactured Parts through Build Parameter Modifications.” *Journal of Manufacturing Science and Engineering* 136.6 (2014)

Hossain, Mohammad Shojib, Jorge Ramos, et al. “Improving Tensile Mechanical Properties of FDM-Manufactured Specimens via Modifying Build Parameters.” *International Solid Freeform Fabrication Symposium: An Additive Manufacturing Conference. Austin, TX*. Vol. 2013. 2013. 380–392. *Google Scholar*.

Joe Lopes, Amit, Eric MacDonald, and Ryan B. Wicker. “Integrating Stereolithography and Direct Print Technologies for 3D Structural Electronics Fabrication.” *Rapid Prototyping Journal* 18.2 (2012): 129–143.

Kadara, Rashid O. et al. “Manufacturing Electrochemical Platforms: Direct-Write Dispensing versus Screen Printing.” *Electrochemistry Communications* 10.10 (2008): 1517–1519.

Kim, Chiyen et al. “Cooperative Tool Path Planning for Wire Embedding on Additively Manufactured Curved Surfaces Using Robot Kinematics.” *Journal of Mechanisms and Robotics* 7.2 (2015).

Lansford, Tom. “3D Printer Carves Out Niche for Big Parts > ENGINEERING.com.”

Li, B., P. A. Clark, and K. H. Church. “Robust Direct-Write Dispensing Tool and Solutions for Micro/Meso-Scale Manufacturing and Packaging.” (2007): 715–721. *Silverchair*.

Louise McGinley, Emma et al. “Effects of Surface Finishing Conditions on the Biocompatibility of a Nickel–chromium Dental Casting Alloy.” *Dental Materials* 27.7 (2011): 637–650.

Macdonald, Eric et al. “3D Printing for the Rapid Prototyping of Structural Electronics.” *IEEE Access* 2 (2014): 234–242.

Medina, Frank et al. “Hybrid Manufacturing: Integrating Direct-Write and Stereolithography.” *Proceedings of the 2005 Solid Freeform Fabrication. Journal of Manufacturing Science and Engineering* (2005). *Google Scholar*.

Navarrete, Misael et al. *Integrated Layered Manufacturing of a Novel Wireless Motion Sensor System with GPS*. DTIC Document, 2007. *Google Scholar*.

Navarrete, Misael. "Three-dimensional electronics packaging integration of stereolithography and direct print" (January 1, 2009). *ETD Collection for University of Texas, El Paso.* Paper AAI1465262. http://digitalcommons.utep.edu/dissertations/AAI1465262

NiChrome - Nickel Chromium Alloys. http://nickel-alloys.net/nickel_chrome_alloys.html.

Pudas, Marko et al. “Gravure Printing of Conductive Particulate Polymer Inks on Flexible Substrates.” *Progress in Organic Coatings* 54.4 (2005): 310–316. *ScienceDirect*.

Pudas, Marko, Juha Hagberg, and Seppo Leppävuori. “Gravure Offset Printing of Polymer Inks for Conductors.” *Progress in Organic Coatings* 49.4 (2004): 324–335.

Pudas, Marko, Juha Hagberg, and Seppo Leppävuori. “Printing Parameters and Ink Components Affecting Ultra-Fine-Line Gravure-Offset Printing for Electronics Applications.” *Journal of the European Ceramic Society* 24.10-11 (2004): 2943–2950.

Puetz, Joerg, and Michel A. Aegerter. “Direct Gravure Printing of Indium Tin Oxide Nanoparticle Patterns on Polymer Foils.” *Thin Solid Films* 516.14 (2008): 4495–4501.

Ramos-Almeida, Jorge. “The Development of Self-Supported Electromechanical Structures Using Fused Deposition Modeling.” (2013): *Google Scholar*.

Ready, Steven et al. “3D Printed Electronics.” *NIP & Digital Fabrication Conference*. Vol. 2013. Society for Imaging Science and Technology, 2013. 9–12. *Google Scholar*. Web. 31 Jan. 2016.

Roberson, David Adrian. "A novel method for the curing of metal particle loaded conductive inks and pastes" (January 1, 2012). *ETD Collection for University of Texas, El Paso.* Paper AAI3512749. http://digitalcommons.utep.edu/dissertations/AAI3512749

Olivas, Richard I. "Conformal electronics packaging through additive manufacturing and micro-dispensing" (January 1, 2011). *ETD Collection for University of Texas, El Paso.* Paper AAI1494367. http://digitalcommons.utep.edu/dissertations/AAI1494367

Shemelya, Corey et al. “Encapsulated Copper Wire and Copper Mesh Capacitive Sensing for 3-D Printing Applications.” *IEEE Sensors Journal* 15.2 (2015): 1280–1286.

Sridhar, Ashok, Thomas Blaudeck, and Reinhard R. Baumann. “Inkjet Printing as a Key Enabling Technology for Printed Electronics.” *Material Matters* 6.1 (2011): 12–15.

“Stratasys Aims to Build on Success with Latest Production 3D Printer > ENGINEERING.com.”.

Szczech, John B. et al. “Fine-Line Conductor Manufacturing Using Drop-on Demand PZT Printing Technology.” *Electronics Packaging Manufacturing, IEEE Transactions on* 25.1 (2002): 26–33.

“Voxel8: 3D Electronics Printing.” http://www.voxel8.co/.

Wicker, Ryan B., and Eric W. MacDonald. “Multi-Material, Multi-Technology Stereolithography.” *Virtual and Physical Prototyping* 7.3 (2012): 181–194.

Woolf, Lawrence D. “Seeing the Light: The Physics and Materials Science of the Incandescent Light Bulb.” (2002): 30–31.

Xun, Xu (Authored). *Integrating Advanced Computer-Aided Design, Manufacturing, and Numerical Control: Principles and Implementations: Principles and Implementations*. IGI Global, 2009.

Appendix

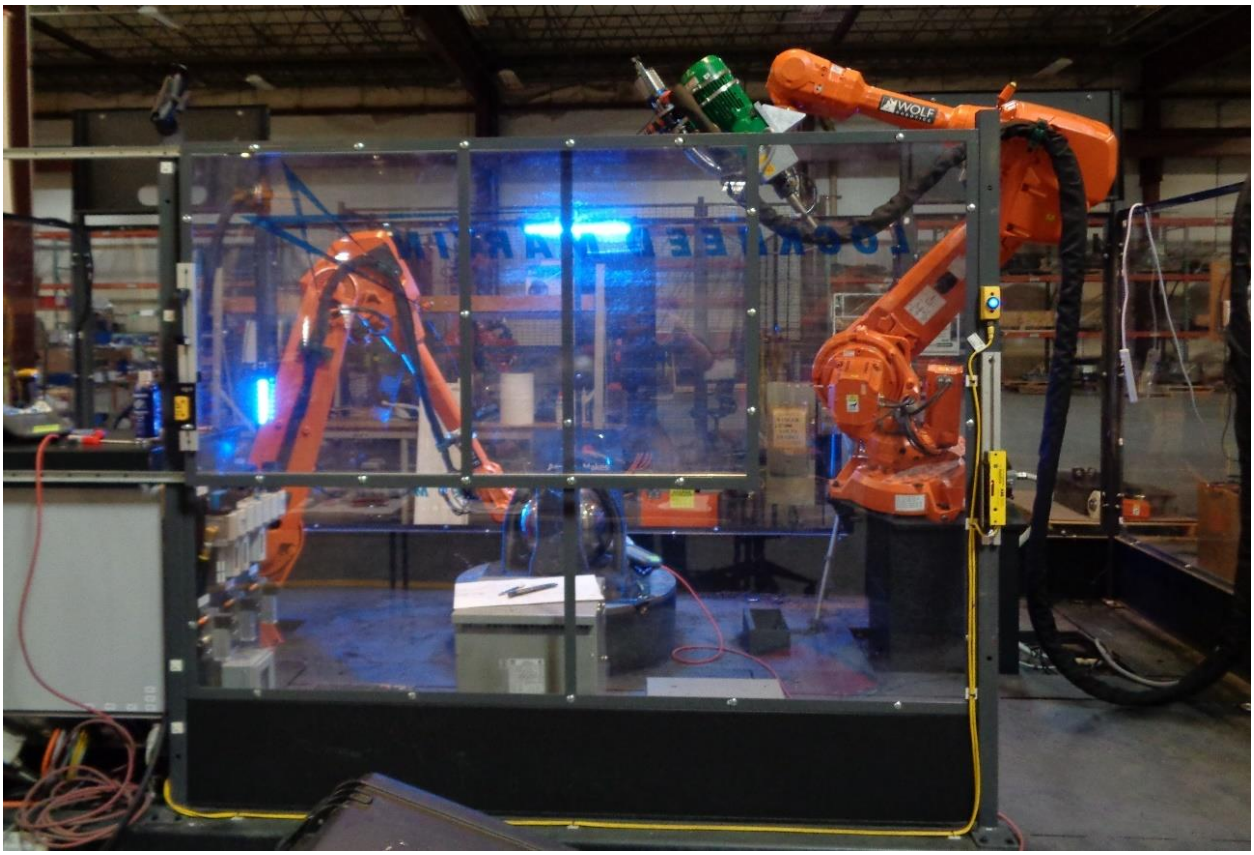

Figure A.1. Photograph of Multi-Robotic Additive Cluster System

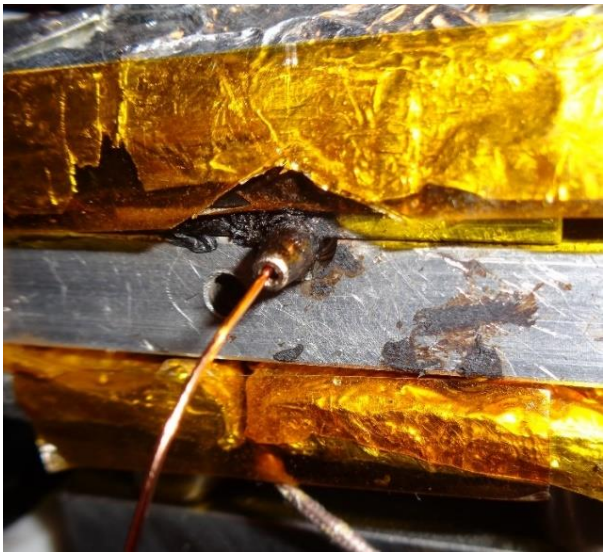

Figure A.2. Photograph of aluminum heated block with visual signs of deterioration

Vita

Daniel Abraham Marquez was born in El Paso, Texas on September 23, 1989 and is the youngest son of Mrs. Irma C. Marquez and Mr. David Marquez Sr. A year after earning his high school diploma at Montwood High school in May of 2008, Daniel began his college career at the El Paso Community College in the Fall of 2009, he later transferred his credits to The University of Texas at El Paso (UTEP). In May 2014, he obtained a Bachelor of Science Degree in Mechanical Engineering. Daniel had an internship as a Product Support Engineer at Azar Mount Franklin Foods where he managed projects assigned to him by the plant manager. Daniel also had an internship working as a Semiconductor Manufacturing Engineer at Texas Instruments where he was awarded the 5S intern award for his work in revamping the forelines on the Phosphorus implanters.

Permanent address: 11613 Stockmeyer Dr.

El Paso, TX, 79936

This thesis was typed by Daniel A. Marquez.